Rational design of a graphene dispersant

A dissertation submitted to the University of Manchester for the degree of Master of Science by Research in the Faculty of Science and Engineering

2016

Junru Zhang

School of Chemistry

Table of contents

Final word count 15,938.

List of figures

List of schemes

List of tables

Glossary of abbreviations

0D	0 Dimension
1D	1 Dimension
1-LG	Single-layer graphene
2D	2 Dimension
2-LG	Double-layer graphene
3-LG	Three-layer graphene
4-LG	Four-layer graphene
AFM	Atomic force microscopy
CVD	Chemical vapour deposition
DMF	N-dimethylformamide
FWHM	Full width at half maximum
GICs	Graphite intercalation compounds
GO	Graphene oxide
HOPG	Highly Ordered Pyrolytic Graphite
HSP	Hansen solubility parameters
l	Path length
LPE	Liquid phase exfoliation
N	Number of graphene layers
NDI-1	N,N'-bis-[2-(ethanoic acid sodium)]-1,4,5,8-naphthalene diimide]
NDI-2	N,N'-bis-[2-(ethanesulfonic acid sodium)]-1,4,5,8-naphthalene diimide]
NMP	N-methyl-2-prrolidone
PBBA	Perylene-based bolaamphiphile
PVP	Pilyvinyprrolidone
Py-2SASS	6,8-Dihydroxy-1,3-pyrenedisulfonic acid sodium salt
Py-3SASS	8-Hydroxypyrene-1,3,6-trisulfonic acid tri sodium salt

Py-4SASS	Pyrene-1,3,6,8-tetrasulfonic acid tetrasodium salt
Py-C_4-SASS	Sodium 4 -(pyren-1-yl) butane-1-sulphonate
Py-SASS	1-Pyrenesulfonic acid sodium salt
rGO	reduced Graphene oxide
SC	Sodium cholate
SDBS	Sodium dodecylbenzen sulfonate
SEM	Scanning electron microscope
SLG	Single layer graphene
SWCNT	Single wall carbon nanotube
TEM	Transmission electron microscopy
TGA	Thermogravimetric analysis
THF	Tetrahydrofuran
UV	Ultraviolet
Y_M[%]	Yield by SLG percentage
Y_w[%]	Yield by weight
Y_{WM}[%]	Yield by SLG weight percentage
ε	Extinction coefficient

Abstract

In this work a novel pyrene based stabiliser has been synthesised in order to increase the production of higher quality graphene in aqueous liquid phase exfoliation. A comparative investigation of liquid phase exfoliation of graphene in water by using designed pyrene stabiliser sodium 4-(pyren-1-yl)butane-1-sulphonate (Py-C_4-SASS) and commercially available 1-pyrenesulfonic acid sodium salt (Py-SASS). The graphene dispersion produced with the novel stabiliser (Py-C_4-SASS) achieves a high concentration of ~1 mg mL^{-1}. In comparison to the commercially available stabiliser (Py-SASS) which produces a dispersion 0.4 mg mL^{-1} under the same experimental conditions. Raman spectroscopy shows both graphene dispersions contain few layer graphene flakes, however the flake size distribution shows that with Py-C_4-SASS as the exfoliation agent the dispersion produces larger graphene flakes (~ 0.4 μm) compared to the Py-SASS graphene dispersion (~ 0.2 μm). A conductivity test is performed to compare the sheet resistance of two graphene inkjet-printed patterns, the results show that the pattern produced from Py-C_4-SASS dispersions has lower sheet resistance (~ 83.76 kΩ/sq) compared to the Py-SASS graphene dispersions(~ 170.21 kΩ/sq). These results suggest that the newly designed stabiliser Py-C_4-SASS enhances the performance in assisting with the liquid phase exfoliation of graphene in water compare to the commercially available stabiliser Py-SASS. This might be because the insertion of a butyl spacer between pyrene aromatic unit and sulfonic acid sodium group could let the hydrophilic group and aromatic moiety of this molecule work more independently.

Declaration

Work undertaken in collaboration with other researchers has been attributed in the text. Computational PMF studies of pyrene stabilisers included herein section (2.3 and 3.1) and the synthesis of pyrene stabiliser Py-C4-SASS included herein (section 2.4 and 3.2) were also included in the PhD thesis (University of Manchester) of Kane Heard (Stephen Yeates group). Work undertaken in the Raman and SEM characterisation of graphene dispersion included herein (section 2.7, 3.5-1 and 3.5-2) will also be included in the PhD thesis (University of Manchester) of Cian Bartlam (Aravind Vijayaraghavan group). No other portion of the work referred to in the thesis has been submitted in support of an application for another degree or qualification of this or any other university or other institute of learning.

Copyright

i. The author of this dissertation (including any appendices and/or schedules to this dissertation) owns certain copyright or related rights in it (the "Copyright") and s/he has given The University of Manchester certain rights to use such Copyright, including for administrative purposes.

ii. Copies of this dissertation, either in full or in extracts and whether in hard or electronic copy, may be made only in accordance with the Copyright, Designs and Patents Act 1988 (as amended) and regulations issued under it or, where appropriate, in accordance with licensing agreements which the University has entered into. This page must form part of any such copies made.

iii. The ownership of certain Copyright, patents, designs, trade marks and other intellectual property (the "Intellectual Property") and any reproductions of copyright works in the dissertation, for example graphs and tables ("Reproductions"), which may be described in this dissertation, may not be owned by the author and may be owned by third parties. Such Intellectual Property and

Reproductions cannot and must not be made available for use without the prior written permission of the owner(s) of the relevant Intellectual Property and/or Reproductions.

iv. Further information on the conditions under which disclosure, publication and commercialisation of this dissertation, the Copyright and any Intellectual Property and/or Reproductions described in it may take place is available in the University IP Policy (seehttp://documents.manchester.ac.uk/display.aspx?DocID=487), in any relevant Dissertation restriction declarations deposited in the University Library, The University Library's regulations (see http://www.manchester.ac.uk/library/aboutus/regulations) and in The University"s Guidance for the Presentation of Dissertations."

Acknowledgements

First and foremost I must thank my supervisors Dr. Peter Quayle and Professor Stephen Yeates for giving me the opportunity to undertake this MSc research study and for their impeccable support and supervision throughout.

I owe special thanks to Dr. Kane Heard for his coaching, advice, and assistance through this year. I also like to thank the collaborator of this project Cian Bartlam for helping me on the characterisation of graphene dispersions. I thank Dr. Adam Parry for doing the AFM analysis and proof reading my thesis. I thank Fiona Porter for doing the grammar proof reading of my thesis.

I thank my beloved family for their unconditional support and love in my life; I would not have the opportunity to start my further study journey in the UK without them. I would also like to thank everyone in OMIC that have been so helpful to me and making my time in Manchester so fantastic and full of surprises. Moreover, I have an extra special thanks to my best friend Miss Xi Huang, my sun and star, for providing me with unfailing support and continuous encouragement throughout my years of study and through the process of researching and writing this thesis. Finally, I would like to thank all my friends and classmates making my time in the UK so colourful and amazing.

1. Introduction

Carbon is one of the key elements of the world. It exists in a variety of allotropes. Diamond is the hardest material while graphite is the softest. In recent decades many new allotropes have been discovered, such as, fullerenes (0D, 0 dimension), single wall carbon nanotube (1D, 1 dimension), carbon nanofibers, and the latest discovery graphene (2D. 2 dimension) (**Fig. 1**).

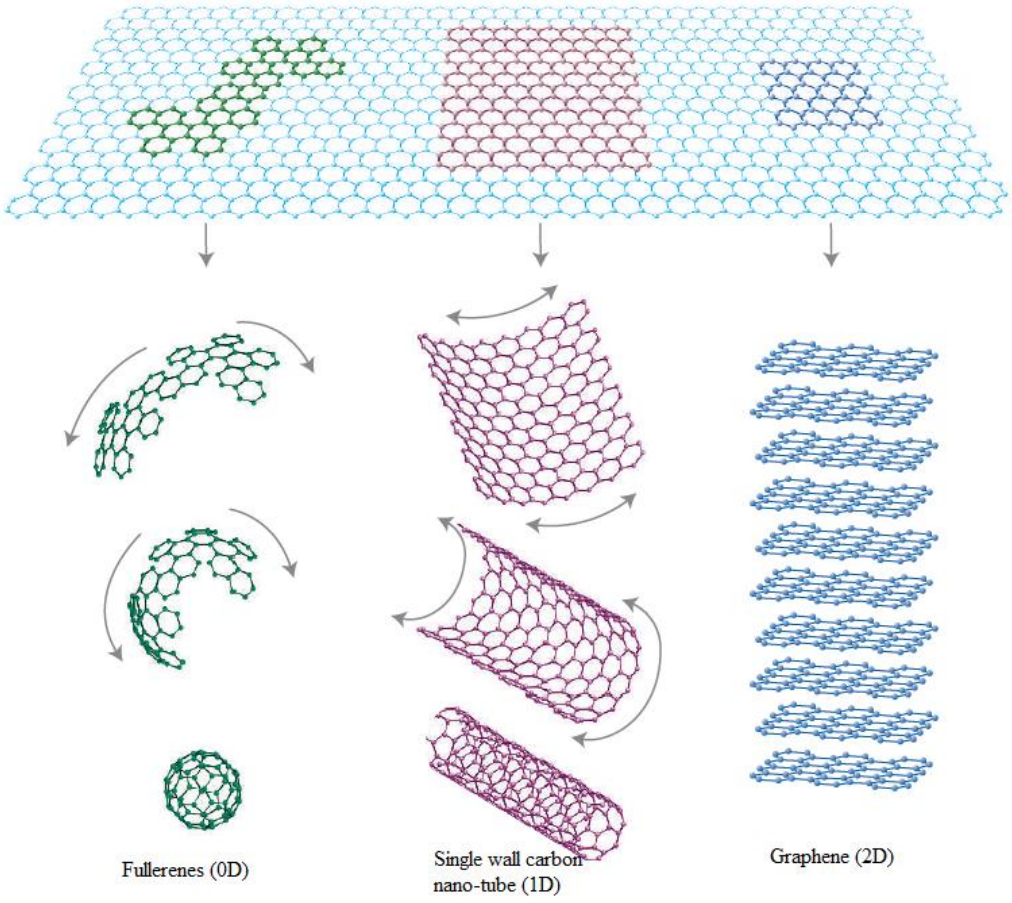

Figure 1: Graphene (2D) material could be wrapped up into (0D) Fullerenes, rolled into (1D) nanotube or stacked into 3D graphite. Adapted from ref. 2

Although as early as the 1940s, it has been suggested that the isolated graphite layer might have extraordinary electronic characteristics[1] it was not proved to be true until 60 years later when Novoselov and Geim, used Scotch tape to isolate single layer graphite.[2]

Graphene is a single atomic layer of graphite with sp^2-bonded carbon atoms arranged in a honeycomb lattice. As shown in **Fig.1**, the graphene could be wrapped up into 0D fullerens, and rolled into 1D nanotubes. These isolated graphitic layers were found to display other remarkable properties, such as high charge carrier mobility (> 2×10^5 cm^2 V^{-1} s^{-1} at an electron density of 2×10^{11} cm^{-2})[3-6], very high thermal conductivity (over 3000 W mK^{-1})[7], exceptional Young modulus values (>0.5-1 TPa), large spring constants (1-5 N m^{-1}) and high surface area (400-700 m^2g^{-1}). [8-13] With these amazing characteristics, graphene has become one of the most attractive materials for many potential commercial applications, including gas and energy storage,[13, 14] as well as micro- and optoelectronics.

This section will discuss the most significant results in liquid phase exfoliation of graphene achieved in the last decade. The review focuses on the exfoliation agent, exfoliation method and the resulting graphene quality (flake size, defects, number of layers) and quantity (miligrams per litre or millilitre of solvent used).

First, the mechanism of the exfoliation will be introduced, then the characterisation method for graphene will be described, and finally a variety of significant liquid phase exfoliation techniques will be introduced and discussed.

1.1 Synthesis methods

There are two major routes to synthesise graphene depending on the nature of the starting material, "bottom up" and "top down". (**Fig. 2**) The methods which use a carbonaceous gas source to synthesise graphene are the bottom up route, while those methods which break-up the layers of graphite solid to form graphene sheets are the top down routes.

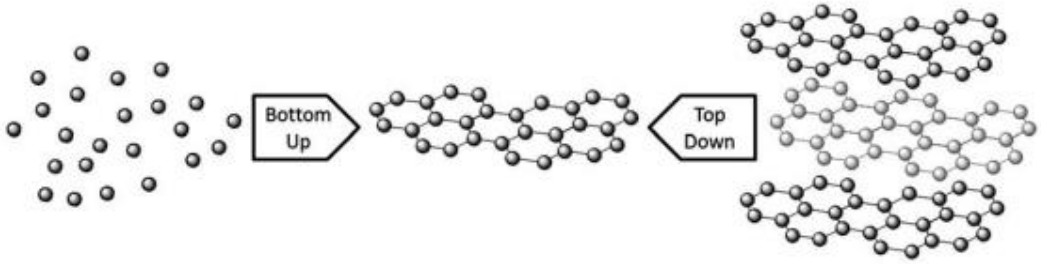

Figure 2: Bottom up and top down routes to synthesise graphene. Adapted from ref. 15

1.1-1 Bottom up methods

In the bottom up route, the most important methods are epitaxial growth on silicon carbide (SiC) and chemical vapour deposition (CVD)[15].

Epitaxial growth on silicon carbide can form single and few layer graphene on SiC *via* silicon sublimation from the SiC surface and the subsequent graphitisation of the excess of carbon atoms left behind.[16] However, this method requires expensive specialised equipment and the size of the graphene is limited by the size of SiC terrace.[17] Alternatively, in chemical vapour deposition (CVD), graphene can be grown on a metal substrate *via* pyrolysis of carbonaceous sources at high temperatures. In this method, transition metals such as copper and nickel are often used due to their catalytic properties.[18] CVD can not only produce single and few-layer graphene, but is also capable of forming large single-layer graphene (~50000 μm).[19] However, for certain applications, the as-obtained graphene has to be transferred to other substrates, and during this process, the graphene sheets can be damaged and become contaminated.[17]

1.1-2 Top down methods

In the top down methods, the graphene is produced by breaking the layers of graphite. It is known that the *d*-spacing between stacked parallel layers in bulk graphite is 0.34 nm. The binding energy between layers is ~ 60 – 72 meV[20] and overcoming this force is the key to successful exfoliation.

Micromechanical cleavage, exfoliation of graphite intercalation compounds (GICs), arc discharge, unzipping carbon nanotubes, graphene oxide exfoliation, and solvent-base exfoliation are the most important top down methods. Micromechanical cleavage, the method which led Novoselov and Geim to win the Nobel prize in 2010 [21, 22], is achieved using an adhesive tape (Scotch tape) to cleave graphene sheets from graphite. Although this is a simple and easy method to produce few layer graphene, it suffers a noticeable disadvantage that large quantities of graphene cannot be produced in short time.[17] Exfoliating graphite intercalated compounds (GICs) by either the solvent-assisted, thermal assisted or microwave radiation assisted method is another effective method.[17] Moreover, physical methods (plasma etching [23, 24] and laser irradiation [25]) could also synthesise graphene.

Recently, the exfoliation of graphene oxide, followed by reduction to graphene (reduced graphene oxide, rGO) has received a lot of attention. During the oxidation process of graphite, the distance between the adjacent layers is expanded by inserting oxygen containing functional groups such as hydroxyl and epoxide to the graphitic layers. It increases the d-spacing between two layers from 0.34 nm to approximately 0.7 nm,[26] which has the effect of lowering the van der Waals attraction, thus making the exfoliation process more efficient to produce pristine graphene. [27] [28] However, this method has a very obvious disadvantage which is the electronic properties of the resulting material are degraded during the aggressive oxidation process, and so far, none of the current methods can fully remove the defects from rGO.

Finally, ultrosonication-assisted exfoliation of graphite in solution has been considered as an alternative to produce high-quality and large quantities of graphene. The shear forces and cavitation, present during ultrosonication, act on the bulk material and induce exfoliation. It can be carried out in organic solvents such as (e.g. N-methyl-2-prrolidone (NMP) and N-dimethylformamide (DMF),[29] which have been shown to have favourable surface energies for exfoliation, or in aqueous solution with the addition of small molecule or polymeric organic stabilisers.[30] The function of the organic solvents and stabilisers is to maintain stable graphene dispersion in the solvent. Organic molecules could provide repulsive steric forces between exfoliated sheets, preventing aggregation or re-association while stabilisers adsorb to the graphite layers resulting in stable colloidal graphene suspension.[31]

1.2 Characterisation methods

For liquid phase exfoliated graphene it is necessary to characterise both the quantity and quality to determine the exfoliation yields. There are three different ways to define the yield of LPE: the yield by weight Y_W [%], the yield by single layer graphene (SLG) percentage, Y_M [%] and the yield by SLG weight, Y_{WM} [%].[32] Among these three methods, Y_{WM} [%] is rarely reported since its determination is very time consuming, even though it is more accurate.

The yield by weight Y_W [%], is the ratio between the weight of graphitic material in the dispersion and the starting graphite flakes. Therefore the estimation of concentration C (mg ml^{-1}) of the graphitic material in the dispersion is vital. The concentration is often determined *via* UV-Vis spectroscopy by using the Beer-Lambert Law: $A = \varepsilon cl$, where A is the absorbance, l (m) is the path length of the cuvette, and ε (L g^{-1} m^{-1}) is the extinction coefficient. The extinction coefficient ε is determined using the absorbance of known concentration graphene dispersions. The mass of graphene in the dispersion is measured by

filtering a known volume dispersion (*via* vacuum filtration) onto a filter of known mass[29], and measuring the resulting mass using a microbalance.

Y_M[%] is the ratio between the number of SLG and the total number of graphitic flakes in the dispersion. For determining the number of graphene layers (N), transmission electron microscopy (TEM) and atomic force microscopy (AFM) are the most frequently used techniques. In TEM, analysing the flake edges or electron diffraction patterns is analysed to calculate N, while in AFM measuring the height of the deposited flakes gives an estimate of the number of single and few layer flakes. [33]

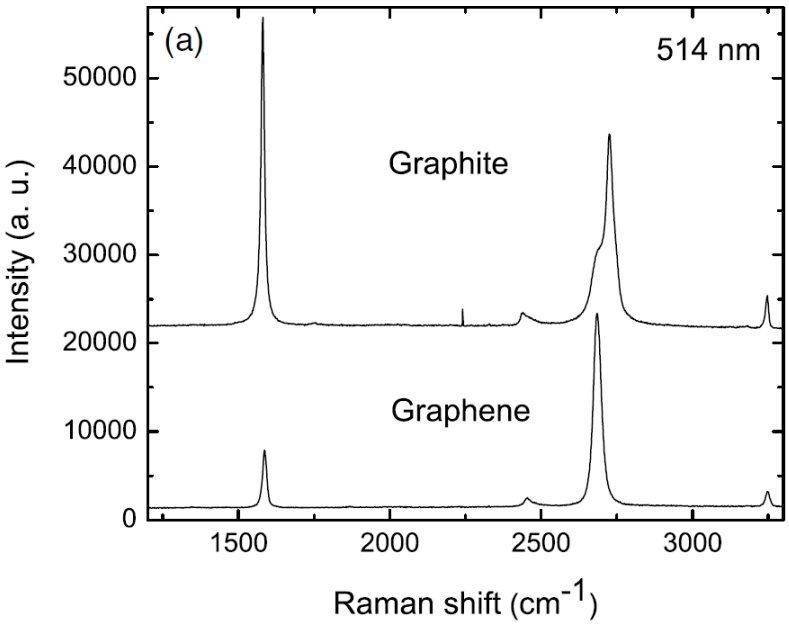

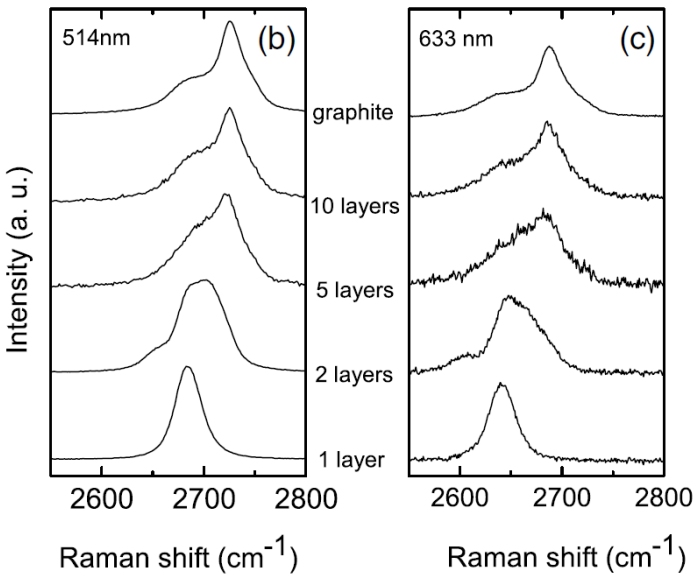

Figure 3: (a), (b) and (c) Raman spectra of graphene and graphite. (Adapted from ref. 30)

Finally, Raman spectroscopy is used to further confirm the result from TEM and AFM. Raman spectroscopy can capture graphene's unique electronic structure in order to determine the number of graphene layers (N). As shown in **Fig.3**, a single layer graphene Raman spectrum has an intense G band at ~ 1580 cm^{-1} and a band at ~ 2700 cm^{-1} , named G' band or 2*D* band. Furthermore, at room temperature, it exhibits a single Lorentzian feature with a full width at half maximum (FWHM) of 24 cm^{-1}, and the intensity of the 2*D* band is much larger than the G peak.[34] Moreover, in defected graphene, a *D* band at ~ 1350 cm^{-1} will show up in the spectrum, yet sometimes the edge effect of graphene will also cause the appearance of a D band. Among these bands, the shape, width and position change of 2*D* band reflect the change in the number of layers of graphene. The 2*D* band of multi-layer graphene is broader and up-shifted relative to the single layer graphene's. However, Raman spectroscopy can hardly distinguish more than 5 layer graphene from bulk graphite. (**Fig. 3 (b) and (c)**) [33]. Therefore, more than one technique is needed for analysing the exfoliation yield.

1.3 Organic solvent assisted sonication

As mentioned previously, the distance between stacked parallel graphene layers in bulk graphite amounts to 0.34 nm. To make complete exfoliation is difficult even though the van der Waals attractions among adjacent layers are weak. Brodie[35] made the first attempt to produce single layer graphene sheets by exfoliation in 1859. Since then, many scientists have tried to make large-scale production of graphene using this method. One of the most effective and straightforward methods to reduce the strength of the van der Waals attractions is liquid immersion, where the potential energy between adjacent layers is contributed by the dispersive London Interactions, which in the presence of a solvent are significantly reduced with respect to vacuum. For graphite, the surface energy is defined as the energy per unit area required to overcome the van der Waals forces when peeling two sheets apart. Therefore, the minimal energy cost of exfoliation for solvent should match the surface energy of graphene. Hernandez *et al*[29] dispersed graphite in a wide range of solvents. It was found that solvents with surface tension (γ) in the region of 40 -50 mJ m^{-2} are suitable for successful graphene exfoliation, since they minimise the interfacial tension between the solvent and the graphene. The graphene film produced by this method could achieve high conductivity (~ 6500 Sm^{-1}). Although suitable solvents were found, the concentration of the graphene dispersion was quite low (< 0.01 mg mL^{-1}). Such a low concentration makes many applications impractical. In 2010, Khan *et al*[36] extended the sonication time and obtained higher concentration graphene dispersions. In this method, the graphite was bath sonicated for up to 460 h using NMP as the organic solvent. After centrifugation (500 rpm, 45 min), a yield of ~ 1 mg mL^{-1} of graphene dispersion was obtained, and over 90% of the graphene flakes were less than 5 layers. Although the concentration was increased, the usefulness of this method is low owing to the long sonication times. The same group of researchers also developed a method to prepare high concentration graphene dispersions for graphene/polyurethane composites. In

this method, graphene was bath sonicated in DMF for 150 h, and the dispersion was filtered through a nylon membrane. The membrane plus graphene was immersed in either DMF or THF and bath sonicated for a further 60 min. During the sonication, the graphene on the membrane came off and re-dispersed in the solvent. This new graphene dispersion had a concentration as high as 20 mg mL^{-1}.[37] In 2011, they tried to improve this method by bath-sonicating graphite powder in NMP to give partially graphitic dispersions. Then after removing any un-exfoliated graphite by centrifugation, the exfoliated graphene was collected by filtration. Re-dispersion of this exfoliated material resulted in good quality dispersions with concentrations of at least 63 mg $mL^{-1.}$ However, the stability of this graphene dispersion was poor because after over 200 h of sedimentation, the concentration dropped to 35 mg mL^{-1}. The dispersion contained good quality graphene flakes with an average of three layers and lateral sizes of ~1 μm × 0.5 μm. The authors believed that these graphene flakes could be applied in areas such as rheology and the dispersions showed liquid crystalline behaviour. [38]

Besides from re-dispersing exfoliated graphene to improve the graphene concentration in organic solution, Liu et al[39] added poly(styrene-co-butadiene-co-styrene) (SBS) to graphite, and reported an increase in the concentration of graphene, which they attributed it to the graphene sheets being stabilised through the π-π stacking with the polystyrene (PS) chains. Although the authors claimed that they produced highly soluble SBS-assisted-graphene, they did not report the concentration of the dispersion, and the quality of their graphene sheets were not ideal.

Research has been done to improve the concentration of graphene dispersions by pre-treating the starting material (e.g. graphite powder). In 2013, Barwich *et al*[40] pre-sonicated graphite powder in solvent (NMP) and non-solvent (water) for 6 h. It usually took 90 min of tip-sonication of graphite in NMP to achieve a concentration of 1 mg mL^{-1}, but for pre-treated graphite, 1 mg mL^{-1} could be achieved in a much shorter time, and both pre-treatment

solvents have their own advantages. Such as for water, the collection of the treated powder was easy because the graphene produced sediments out of dispersion under gravity; however for NMP, the concentration of the graphene dispersion was considerably higher. The authors suggested that the pre-treatment could be chosen depending on the details of the application.

In 2014 Hossain *et al* [41] developed another pre-treated method by pre-heating the pristine graphite at 900 ºC for 5 h in a sealed bath under high pressure and a N_2 environment, followed by cooling to 250 ºC at a speed of 4 ºC/min. This preheated graphite was then stirred with NMP at 180 ºC – 190 ºC for 25 min under N_2 gas, then cooled to room temperature. The sample was then tip-sonicated for 3 h, and the supernatant was collected after settling for 140 h. The obtained concentration of graphene dispersion was 5.25 mg mL^{-1} with a yield by weight of 14%. It was suggested that this pre-thermal treatment expanded the graphite layers and enabled the preparation of single-, double-, and multi-layer graphene sheets upon sonication in an organic solvent. Although the final concentration of graphene dispersion was very high (5.25 mg mL^{-1}), this method only let the post-sonication sample settle for a few days to sediment the big graphite flakes instead of using centrifugation to thoroughly remove unexfoliated graphitic material. Thus, the high concentration might not be very reliable comparing to other reports.

Zheng *et al*[42] developed a low-cost, environmental friendly, and oxidation free method called "salt-assisted direct exfoliation of graphite". In this method, graphite and inorganic salt such as NaCl and $CuCl_2$ were stirred together, and the mixture dried by evaporation. During this process, salt ions entered and precipitated or crystallised within the inner layer spaces of graphite as the solution became supersaturated during water evaporation. The crystallised salt ions expand the graphite layers dramatically, so that the further exfoliation is easier to conduct. The resulting residue was added to an organic solvent such as NMP, ethanol, DMF or toluene and sonicated at low power for 2-3 h. The concentration of the graphene dispersion

could achieve 0.11 mg mL^{-1}. The concentration was not improved dramatically though and the obtained graphene dispersion contained 86% few-layer graphene sheets with lateral sizes as large as 210 μm^2. With such a large lateral size these graphene dispersions have great potential for the manufacture of high-performance electronic devices and graphene-reinforced composites.

Solvents whose surface tensions are close to 40 mJ m^{-2} e.g. NMP, DMF etc. are suitable for direct liquid phase exfoliation of graphene, however have some significant drawback for large-scale production. These solvents are toxic with high boiling points which limit their viability in industrial application. Therefore, it is necessary to search for an alternative solvent which could overcome these drawbacks. An ideal option is to use volatile solvents to stabilise exfoliated graphene. Choi *et al*[43] exfoliated graphene directly in 1-propanol, yet only achieved a dispersion with a concentration of 0.025 mg mL^{-1}. In 2012, Zhang *et al*[44] presented a method to transfer exfoliated graphene in ethanol by solvent exchange, but these procedures gave very low concentration of graphene. Although it seems impossible to perform direct graphene exfoliation in poor solvents, the theory of Hansen solubility parameters (HSP) has testified that a given solute can be dissolved in a designed mixture of even two non-solvents.[45] Therefore, exfoliating graphite into graphene in the solvent mixture directly might be possible. In 2012, Yi *et al*[46] exfoliated graphite flakes in water-alcohol mixtures. The maximum concentration of the graphene dispersion was 0.020 mg mL^{-1}, with a yield [Y_W] of ~10%. In addition, their resultant graphene dispersion contained ~ 8 % mono-layers and 86 % few-layer graphene, and the graphene flakes were mostly high quality without defects. This research showed that a binary volatile solvent system could exfoliate graphene, but increasing the concentration of the dispersion still remained a problem. In 2016 Zhang *et al*[47] developed a process to exfoliate graphene in a ternary-solvent mixture (acetone/tetrafydrofuran/water) according to HSP theory. This process increased the

concentration to several mg mL^{-1}, which was an improvement compared to the binary solvent system. Ideally, volatile solvents would be a good alternative for liquid phase exfoliation of graphite; however, these previous attempts showed that even though it is possible to perform successful exfoliation, the yield is far too low compared to the high-boiling point organic solvents, such as NMP.

1.4 Stabiliser-assisted exfoliation

Water is non-toxic, environmental friendly and abundant, making it the ideal choice for LPE of graphite. Furthermore, graphene in water makes the formation of biocompatible graphene based material for biomedical application possible. However, the hydrophobic nature and the unsuitable surface energy make it difficult to conduct graphene exfoliation in water. Fortunately, this challenge can be overcome using molecules which are able to stabilise the graphene sheets in the water. Stabilisers adsorb onto the graphene surface which minimises the surface free energy, thus solubilising the sheets in solution.

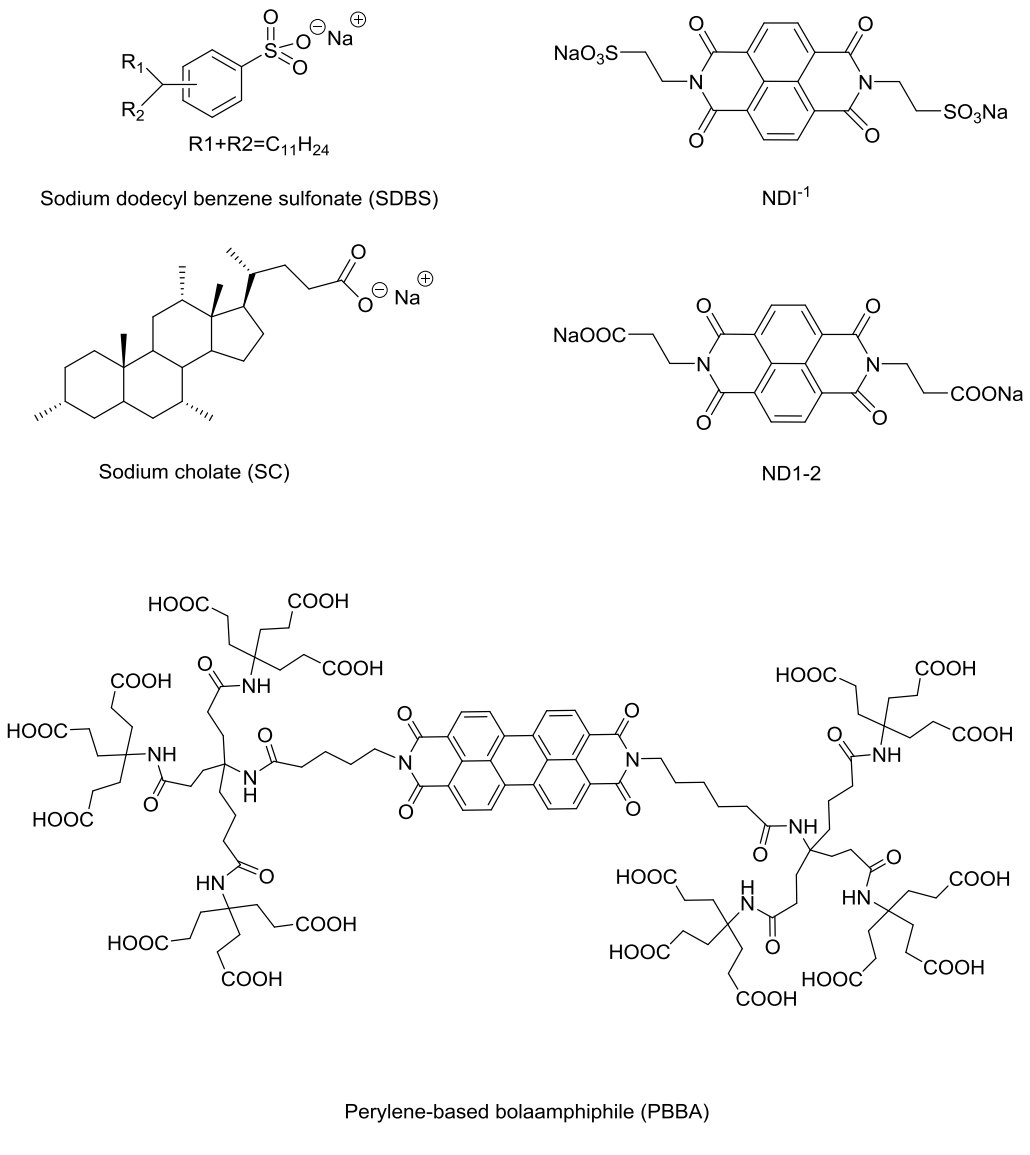

Figure 4: Chemical structures of organic molecules used as surfactants LPE, with their names and corresponding acronyms as used in the text.

In 2009, Lotya[48] and co-workers investigated direct exfoliation of graphite in surfactant/water solutions in a manner similar to surfactant aided carbon nanotube dispersion. In their research, sodium dodecylbenzen sulfonate (SDBS) (**Fig. 4**) was used as surfactant. The observed concentration of resulted graphene dispersion was between 0.002 ~ 0.05 mg mL^{-1}, and it contained large quantities of multilayer graphene with less than 5 layers and smaller quantities of monolayer graphene. Moreover, the dispersion was stable over approximately 6 weeks. Inspired by Lotya's work, Englert *et al*[49] reported a method to produce graphene

dispersion by ultrasonicated graphite with the highly water soluble perylene-based bolaamphiphile PBBA **(Fig. 4)**. There were no defects caused by the sonication or chemicals, so that the entire graphene sheets were intact. The author believed that this method opened the door to inexpensive production, analysis, and manipulation of exfoliated graphene in large quantities for future applications. However, the authors did not discuss the lateral size, the number of layers or the concentration of the graphene dispersions. Therefore the exfoliation efficiency of this method is unknown.

In 2010, Coleman and co-workers[50, 51] demonstrated a low-cost method to produce stable graphene dispersions in water with the addition of sodium cholate (**Fig. 4**), yielding concentrations of up to 0.3 mg mL^{-1}. The resulting graphene dispersion contained about 10% monolayer graphene flakes and up to 80% of flakes with less than 5 layers. They found the conductivity of unwashed graphene film was low (~35 S m^{-1}), yet after removing the residual of surfactant, the conductivity increased significantly to ~ 1500 S m^{-1}. However, this number is still far lower than the previously reported conductivity of the film prepared by using NMP as the exfoliation solvent (~6500 S m^{-1})[29]. The authors believed the residual surfactant may impede the electrical properties of graphene film. Although the conductivity is not satisfactory for applying it in in transparent electrodes, the production process of making these graphene thin films is low-cost and scalable, therefore, this method still have potential.

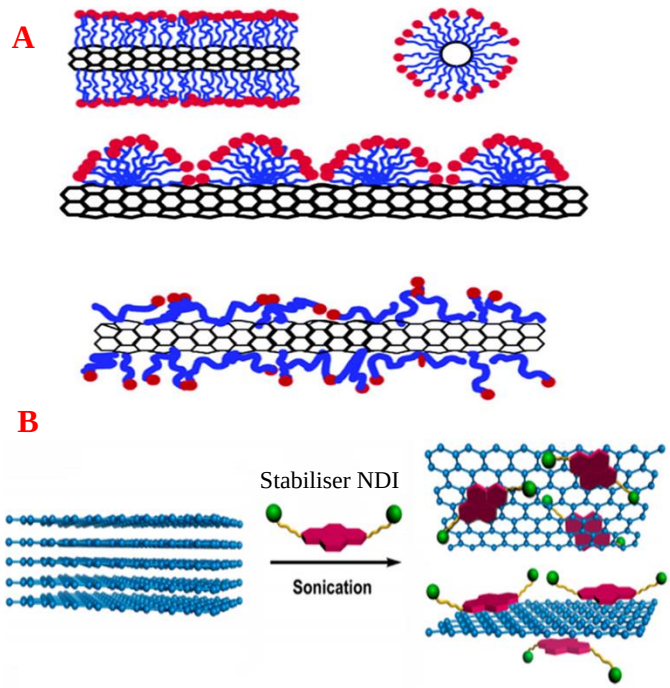

Figure 5: (A) Mechanism when surfactants disperse SWCNT (adapted from ref. 52); (B) Mechanism of stabilisers disperse graphene (adapted from ref. 53)

According to the literature, exfoliating graphite in water with the aid of a surfactant is feasible. It is noteworthy that most of the surfactants reported for graphene dispersion are borrowed from the field of single-walled carbon nanotube (SWCNT) dispersion. The ideal stabiliser (or surfactant) of SWCNT and graphene share similarity as they both need to have aromatic unit to interact with graphitic material and polar unit to stabilise them into the liquid phase. However, SWCNT is a material with a curved surface while graphene is a material with a flat surface; therefore the mechanism of dispersing them in water is different. The mechanism of surfactant in dispersing the SWCNT is similar to dispersion of solid particles (**Fig. 5(A)**)[52]; but the mechanism of stabiliser in dispersing graphene is that the aromatic unit having π-π interaction with graphene sheet meanwhile the polar unit interacting with water **(Fig. 5(B)**[53]. Hence, stabiliser (or surfactant) suitable for exfoliating SWCNT might not always be suitable for exfoliating graphene. Therefore, in 2014, Zhang *et al*[53] designed and

synthesised two novel surfactants, N,N'-bis-[2-(ethanoic acid sodium)]-1,4,5,8-naphthalene diimide (NDI-1) and N,N'-bis-[2-(ethanesulfonic acid sodium)]-1,4,5,8-naphthalene diimide] (NDI-2) (**Fig. 4**) for high-efficient graphene exfoliation. The designed surfactants contained ionic groups covalently bonded to a large, electron-deficient aromatic unit through flexible alkyl spacers. The aromatic unit was designed to attach to the graphene surface *via* π-π interactions, whereas the ionic groups would stabilise the graphene sheets in water. Moreover, the presence of flexible alkyl spacers could ensure the aromatic unit and hydrophilic unit working independently with a synergetic effect. Ultrasonicating these novel surfactants with pristine graphite resulted in a concentration of graphene up to ~5.0 mg mL^{-1}, with about 6% single-layered graphene flakes.

1.4-1 Pyrene stabilisers

From Zhang's investigation,[53] it is clear that stabilisers incorporating aromatic units with organic or inorganic side groups are efficient at stabilising graphene sheets in water. Therefore, pyrene-based derivatives have been suggested as a model polyaromatic hydrocarbon system for graphene stabilisers. Pyrene consists of four fused benzene rings, resulting in a 2D aromatic system suitable as a stabiliser for LPE. The 2-dimensional aromatic core can adsorb to the graphene surface through π-π stacking interactions, while the polar group is able to stabilise the graphene sheets in water.

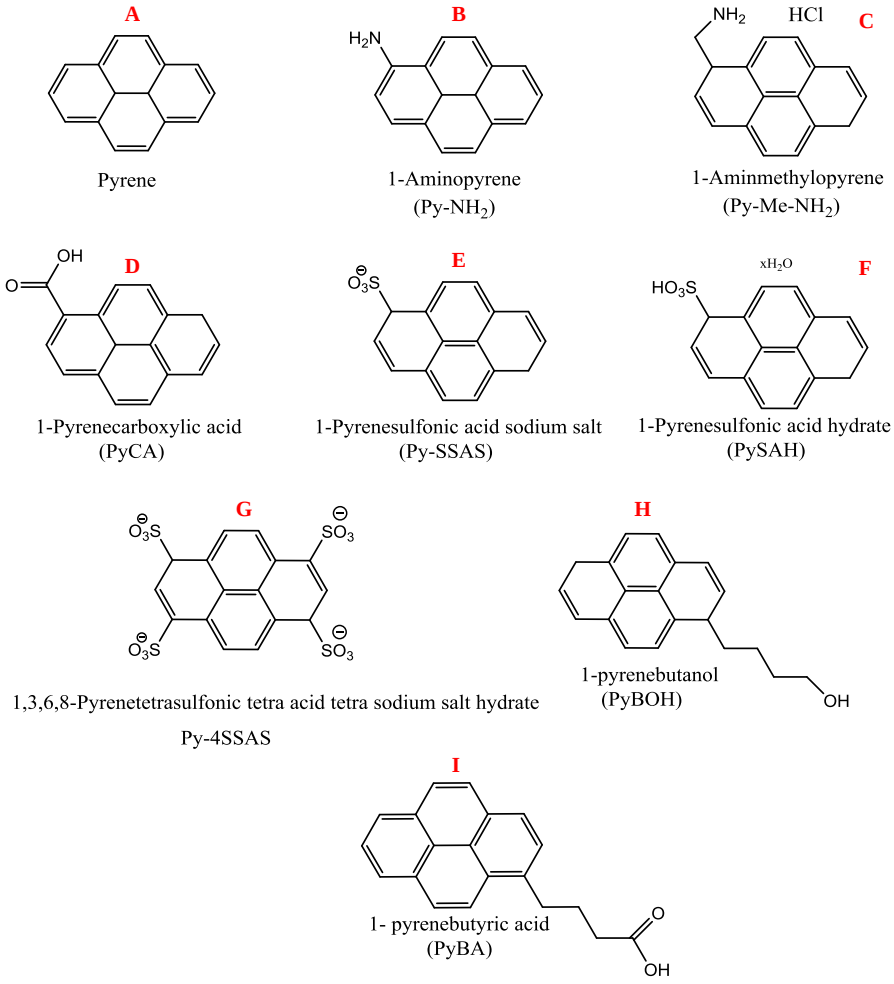

Figure 6: Chemical structures of pyrene derivatives used as surfactants in LPE, with their names and corresponding acronyms as used in the text.

In 2010, An *et al*[54] produced high performance graphene for sensor and ultra-capacitor applications by exfoliating graphite flakes in pyrenecarboxylic acid (PyCA) (**Fig.6A)**. However, neither graphene yield nor the dispersion concentration has been discussed in the report. In a different study by Parviz *et al*,[55] exfoliated graphene was prepared using a series of pyrene derivatives and their ability to obtain high exfoliation yield and dispersion concentration in water was examined. In this investigation, pyrene (Py), 1-aminopyrene (Py-NH_2), 1-amimomethyl pyrene (Py-Me-NH_2), 1-pyrene carboxylic acid (PCA), 1-pyrenebutyric acid (PyBA), 1-pyrenebutanol (PyBOH), 1-pyrenesulfonic acid hydrate (PySAH), 1-pyrenesulfonic acid sodium salt (Py-SASS) and 1,3,6,8-pyrenetetrasulfonic tetra

acid tetra sodium salt (Py-4SASS) (all molecules are shown in **Fig. 6**) were used. It was found that 1-pyrenesulfonic acid sodium salt (Py-SASS) was the most effective stabiliser among all these pyrene derivatives, yielding the concentration of graphene dispersion as high as 0.8-1 mg mL^{-1} whereas the concentration of Py-4SASS graphene dispersion is low (~0.04 mg mL^{-1}). The authors believe it is because the probability of temporary polarisation is reduced due to the symmetric arrangement of the functional group around the basal plane. They also found that having the functional groups with higher electronegativity on the stabiliser are more effective at driving the adsorption of the stabiliser onto the graphene layers. Moreover, the steric effect of pyrene basal plane caused the self-aggregation of pyrene derivatives at high concentration since the distance between the aromatic unit and the functional groups are short, hence the coverage of stabiliser to graphene surface might be decreased. Although the final graphene concentration is high, the researchers here used expanded graphite which is much easier to exfoliate compared to natural graphite. Furthermore, the authors believed that a higher quality and quantity of graphene dispersion could be obtained by using designed graphene stabilisers by manipulating the molecular structures.

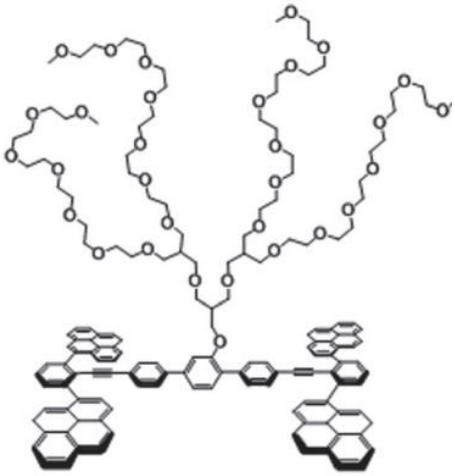

Figure 7: Chemical structure of amphiphile 1.

In 2011, Lee *et al*[56] synthesised an amphiphilic molecule (**Fig. 7**) based on four pyrene units and a laterally-grafted oligoether dendron. For this molecule, the pyrene units can adsorb onto the graphene surface through π-π interactions, while the hydrophilic dendron pulls the graphene surface away to generate hydrophilic outer layers, resulting the graphene sheets to be stabilised in aqueous solution. The graphite powder was sonicated with this amphiphilic molecule in a water and methanol mixture. After centrifugation, the concentration of the resulting dispersion was 1.5 mg mL^{-1}, which was much higher than other reported concentrations of graphene dispersions by direct exfoliation. Moreover, the lateral size of the exfoliated graphene sheets was about 2-4 μm in diameter. Although the resulting concentration of graphene dispersion was high, the LPE was performed in water/methanol mixture rather than pure DI-water. Hence, it might be imprecise for direct comparison with results performed in water only.

Parviz *et al*[55], found that Py-SASS is the best stabiliser among a series of pyrene-based derivatives. Therefore, in 2013, Yang *et al*[57] exfoliated graphite in deionised water by using 1-pyrenesulfonic acid sodium salt (Py-SASS) to further study the nature of Py-SASS in LPE.

In their investigation, a detailed characterisation, both spectroscopic and microscopic was used to analyse the concentration, lateral size, and the defects of the resulting graphene flakes. In addition, they tried to remove any excess Py-SASS on the graphene by centrifugation and re-dispersion in order to gain more accurate measurements. The concentration of the dispersion, after washing, was 0.074 mg mL^{-1}, and about 70 % of the graphene was few-layer. The authors believed that since protein and other biological objects can be easily attached to pyrene, the suspension can be used as inks for printable tattoo-based electro-chemical sensors.

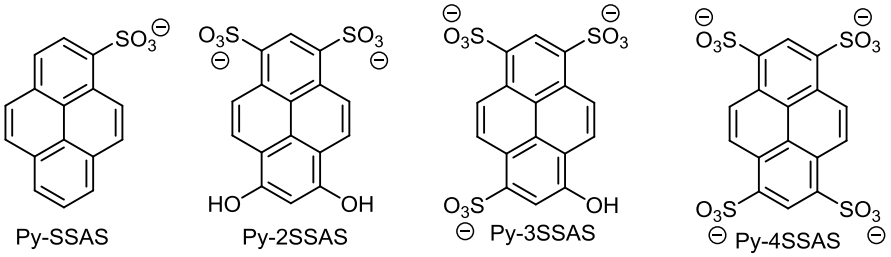

Figure 8: Chemical formula of the four pyrene derivatives

It is known from the previous review that pyrene derivatives are effective stabiliser in liquid phase graphene exfoliation; however the exact details of the interaction between graphene and pyrene are still unclear. Therefore, Schlierf *et al*[58] studied the mechanism of surface adsorption of pyrene derivatives (shown in **Fig. 8**) on graphene, by combining experimental evidence with computational simulations. Potential mean force (PMF) curves indicated that Py-SASS and Py-2SASS have a single global minimum in free energy (face – face stacking on the graphene surface). It is found that as Py-2SASS approaches the graphene surface, the SO_3^- group is pointing away from the graphene surface, but as molecule gets closer to graphene, it starts to slides and orients parallel to the graphene surface. However, Py-3SASS and Py-4SASS show more than one minima on approaching the graphene surface when the molecules tilts from an initial edge on interaction to a fully adsorbed state. The authors

suggest that the asymmetric shape of the stabiliser molecule facilitates the step when the stabiliser approaches the graphene surface and changes its orientation in order to slide into this layer. These results suggest Py-4SASS performs poorly not only just because of the strong steric hindrance effect of four sulfonic groups around the basal plane but also because the symmetric functionalization of the molecule means it only has a weak dipole which cannot facilitate the "sliding" effect as it finally changing to the face-face interaction on the graphene surface.

Although a lot of progress has been made on direct exfoliation of graphite, the removal of the residual stabiliser is poorly understood and often neglected in the literature. However, the removal of both bulk and/or adsorbed dispersant is industrially relevant and has the potential to improve the properties of the graphene (e.g. conductivity). Most reports in the literature used centrifugation and re-dispersion to remove excesses dispersant, and yet this method will usually decrease the final concentrations and large lateral size graphene flakes will be removed during this process as well. In 2016, Irin *et al*[59] studied the removal of residual stabiliser molecules from colloidal graphene solutions. Three methods, dialysis, vacuum filtration, and spray drying were investigated for two different dispersants, polyvinypyrrolidone (PVP), and 1-pryrenesulfonic acid sodium salt (Py-SASS). These two stabilisers were chosen as their mechanisms of stabilisation are different. PVP is a polymer which stabilises graphene by physical adsorption and steric hindrance, while Py-SASS is an aromatic molecule which non-covalently binds to the graphene through π-π interactions and stabilises the dispersion by electrostatic repulsion. Their results showed that vacuum filtration is the most effective method (removing up to ~95 wt%) to remove stabiliser molecules residual. The most significant result in their work is that the dispersion state is not significantly affected by the removal of excess stabiliser because desorption of stabiliser from the graphene surface is slow.

All of these previous investigations showed that pyrene derivatives are suitable for high-efficient, large scale graphene exfoliation in comparison to other literature stabilisers and surfactants. However, modification and the design of novel pyrene-based stabilisers for massive production of graphene dispersions will be the new challenge and direction for the future.

1.5 Conclusion

In the last decade, significant developments have been made for the low-cost liquid phase exfoliation of graphite to produce large quantity, high quality graphene. Final graphene dispersions are stable yet these techniques must still overcome the following problems:

- The yield of single-layer graphene sheets is still relatively low;
- The lateral size of graphene sheets is small;
- Although long sonication time can increase the final concentration of graphene, the graphene can become damaged and the lateral size of graphene flake will decrease;
- The removal of surfactants or stabilisers from the final graphene samples is difficult and of low efficiency.

Therefore, it is important to investigate the design or discovery of efficient and suitable stabilisers or solvent systems to achieve large-scale production of high quality few-layered graphene through liquid phase exfoliation.

From the literature review above, the potential desirable properties of stabiliser in liquid phase graphene exfoliation in water medium could be summarised as follows:

❖ The stabiliser should be amphiphilic, with aromatic core and a polar hydrophilic group. The aromatic unit could have π-π interaction with graphene while hydrophilic group could stabilise the exfoliated graphene flake in water.

- ❖ The hydrophilic group should be isolated away from the aromatic core to ensure that both parts work independently to avoid the steric hindrance effect. A flexible alkyl chain is an ideal spacer for separation.[53]
- ❖ In order to facilitate the "sliding" effect of the molecule into a face – face interaction, the structure of the stabiliser molecule should be asymmetrically functionalised. Additionally, the hydrophilic functional group should be on one side and the molecule should have a dipole moment across the molecule.

1.6 Aims of the project

The aims of this project are to designed and synthesise our new stabiliser according to the previous paper's suggestions and compare its stabilisation ability to graphene to the commercially available stabiliser Py-SASS.

This project has following specific aims:

1. According to Parviz *et al*[55] stabiliser Py-SASS gave the best performance in liquid phase exfoliation of graphene among other pyrene derivatives. Therefore, Py-SASS is used for comparison to our designed stabiliser owing to its lack of alkyl spacer to separate the aromatic unit and hydrophilic unit.
2. For designing the stabiliser for exfoliation, a flexible alkyl spacers is needed between the aromatic core and the hydrophilic group to isolate these two units in order to let them function independently.[53, 55] Therefore pyrene-based amiphilic graphene stabiliser with a SO_3Na group separate from the aromatic core by a butyl chain will be synthesised.
3. Perform liquid phase exfoliation of graphene by using the abovementioned designed stabiliser and a commercially available stabiliser Py-SASS.
4. Compare the ability of exfoliation of these two stabilisers by analysing the quantity and quality of their graphene dispersion.

2. Experimental

2.1 Material

All reactants and reagents were purchased from Sigma Aldrich, Fisher Scientific. Natural graphite flakes were purchased from NGS Naturgraphit GmbH and used without further treatment.

2.2 Characterisation

^{1}H NMR spectra were recorded with using a Bruker Avance III 400. MALDI mass spectra were recorded with a Shimadzu Biotech Axima Confidence spectrometer. Infrared spectra were obtained using a Thermo Scientific Nicolet iS5 spectrometer with an iDS ATR accessory.

UV-vis absorption spectra were recorded on a Varian Cary 5000 UV-vis-NIR spectrophotometer.

The graphene flakes sample was prepared by spin-coating the graphene dispersion (~0.1 mg mL^{-1}) on to a $Si|SiO_2$ substrate at 1200 rpm for 5 minutes.

Raman spectra were acquired using Renishaw InVia spectrometer with a 514 nm laser at 1% power with 10 second acquisition time with 2 accumulations. The data was averaged over 30 points. This was carried out in the WiRE 4.1 software package along with the peak fitting of G, G$^{'}$ and 2D bands.

SEM imaging was performed on a Ziess Ultra at gun voltage 15kV with an InLens detector. AFM images were acquired on a Park XE-100 in non-contact mode using a cantilever with a spring constant of 5 N/m.

2.3 Simulation method

Molecular dynamic simulation was performed by Dr. Flor Siperstein *et al*[60] at the University of Manchester. The detailed simulation procedures are reported in PhD thesis of our group member Dr. K Heard.[61]

2.4 Synthesis of pyrene-based stabiliser

2.4-1 4-(Pyrene-1-yl) butan-1-ol

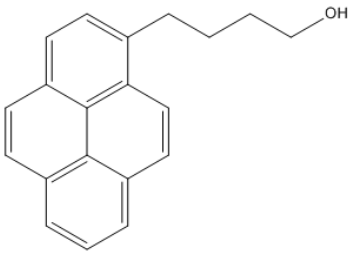

4-(Pyrene-1-yl) butan-1-ol

Prepared by an adaption of a literature synthetic method[62]

1-pyrenebutytic acid (2 g, 6.6 mmol) was added to a three necks round bottom flask 250 mL which was then purged with N_2. The flask was then cooled to 0 ºC by using an ice-water bath, and then the borane tertrahydrofuran (1.0 M) (30 mL, 30 mmol) complex was added dropwise *via* syringe. The mixture was stirred at the 0 ºC for 10 minutes; the ice-water bath was then removed and the reaction stirred at room temperature for a further 10 minutes. The reaction was heated to 60 ºC overnight. After the reaction was cooled to room temperature, 30 mL of methanol was added *via* syringe and stirred for 5 hours. Then potassium carbonate (500 mg, 3.63 mmol) was added and stirred with the mixture for 10 minutes before water (72 mL) was added *via* syringe. The reaction mixture was then extracted with DCM (75 mL). The organic layers were then combined and washed with water (36 mL) and brine (36 mL). After being dried over $MgSO_4$, the mixture was concentrated in *vacuo.* Finally, the crude product

was purified by column chromatography with a graded solvent system from 20% ethyl acetate in petroleum ether to 30% ethyl acetate to yield 58.4% of 4-(pyrene-1-yl) butan-1-ol (1.06 g, 3.86 mmol) as a cream solid/crystal. mp 75-77 °C (lit., 72.5-74.5 °C[62]). δ_H (400 MHz; CDCl3; CHCl3) 1.50 (1 H, s, OH), 1.65 - 1.72 (2 H, m, C-C-H), 1.84 – 1.92 (2 H, m, C-C-H), 3.32 (2 H, t, *J* = 8.0, Ar-C-H), 3.65 (2 H, t, *J* = 6.0, O-C-H), 7.81 (1 H, d, *J* = 8.0, Ar-H), 7.90 – 7.98 (3 H, m, Ar-H), 8.02 - 8.05 (2 H, m, Ar-H), 8.09 (2 H, dd, *J* = 8.0, 4.0, Ar-H), 8.29 (1 H, d, *J* = 12, Ar-H). These data correspond to the literature.[61]

2.4-2 1-(4-Bromobutyl)pyrene

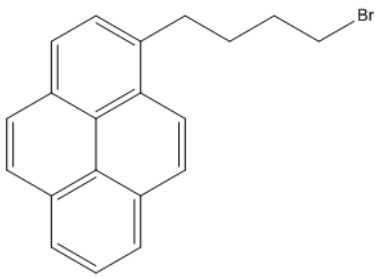

1-(4-Bromobutyl) pyrene

Prepared by an adaption of a literature synthetic method[63]

Tetrabromomethane (1.6 g, 4.83 mmol) and potassium carbonate (0.79, 5.71 mmol) were added to a three necked round bottom flask (100 mL) which was then purged with N_2. 4-(Pyrene-1-yl) butan-1-ol (1.06g, 3.86 mmol) was taken up in dry DCM (18.30 mL) *via* syringe under N_2. The dispersion was then injected into the reaction mixture which was cooled to 0ºC in an ice-water bath. Triphenylphosphine (1.24 g, 4.74 mmol) in dry DCM (7 mL) was added to reaction mixture *via* syringe dropwise. The ice-water bath was then removed and the reaction left stirring at room temperature overnight. The crude product was purified by column chromatography with 10% DCM in petroleum ether solvent system to

yield 26% of the 1-(4-bromobutyl) pyrene (0.34 g, 1.0 mmol,) as a colourless solid. mp 73-74 °C (lit.,71-72 °C[63]). δ_H (400 MHz; CDCl3; CHCl3) 1.94 - 1.99 (4 H, m, C-C-H), 3.29 - 3.32 (2 H, m, Ar-C-H), 3.39 - 3.42 (2 H, m, Br-C-H), 7.80 (1 H, d, *J* = 8.0, Ar-H), 7.91 - 8.00 (3 H, m, Ar-H), 8.05 (2 H, d, *J* = 12, Ar-H), 8.11 (2 H, dd, *J* = 8.0, 4.0, Ar-H), 8.20 (1 H, d, *J* = 12, Ar-H). These data correspond to the literature[61].

2.4-3 Sodium 4-(pyren-1-yl)butane-1-sulphonate (Py-C_4-SASS)

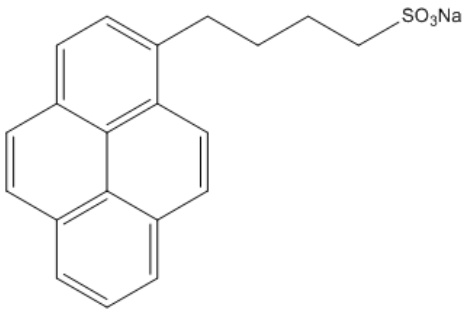

Sodium 4-(pyren-1-yl)butane-1-sulphonate

Prepared by an adaption of a literature synthetic method[61]

$NaSO_3$ (1.5 g, 14.6 mmol) was added to a 2 neck round bottom flask (250 mL) which was then purged with N_2. 1-(4-Bromobutyl) pyrene (0.34 g, 1 mmol) was ground with mortar and pestle, and was then taken up in ethanol (2 mL) with the assistance of sonication. The dispersion was injected into the reaction *via* syringe. Water (20 mL) was also added *via* syringe before the reaction was heated to 100 ºC overnight. After the crude product was concentrated in *vacuo* and trituated with DCM (10 mL), it was recrystallized by using ethanol:water mixture (~1.3:1) (concentrated in *vacuo*). The filtered crystals were washed with ice cold water (10 mL) and DCM (10 mL) to yield 44% sodium 4-(pyren-1-yl)butane-1-sulphonate (0.16 g, 0.44 mmol) as off-white crystal. mp >300 °C. (Lit mp > 300 ºC[61]) δ_H (400 MHz; DMSO) 1.70 – 1.87 (4 H, m, C-C-H), 2.49 - 2.55 (2 H, m, SO_3Na-C-H), 3.30 - 3.34 (2 H, m, Ar-C-H), 7.95 (1 H, d, *J* = 7.9, Ar-H), 8.04 – 8.15 (3 H, m, Ar-H), 8.19 - 8.23

(2 H, m, Ar-H), 8.25 - 8.29 (2 H, m, Ar-H), 8.36 (1 H, d, *J* = 9.14, Ar-H). *m/z* (ESI^-) 697 ($[M - Na + M]^-$, 15%), 337 ($[M - Na]^-$, 100). (ESI+) 743 ($[M + M + Na]^+$, 30%), 383 ($[M + Na]^+$, 100). HR *m/z* (ESI^+) $C_{20}H_{17}NaO_3S$ + Na requires 383.0672, found 383.0688. ν_{max}/cm^{-1} 3530br and 3476br ($SO_3Na•H_2O$), 3040 (Ar C-H), 2934 and 2868 (C-H), 1621, 1604 and 1590 (Ar C=C). These data correspond to the literature.[61]

2.5 Tensiometry

Saturated solutions of stabilisers (Py-C_4-SASS and Py-SASS) were prepared in 10 mL deionised (DI) water. The mixture was heated to 80-90 ºC and stirred for 10 minutes to obtain a suspension. A syringe filter was used to filter the undissolved stabiliser, and the transparent solution was collected as a stock solution of the stabiliser. Furthermore, a 0.1 mg mL^{-1} solution of both stabilisers was prepared and the absorbance of the stabiliser dispersions with a variety of dilutions at λ_{max} was measured. A Beer-Lambert plot was plotted and the extinction coefficients of stabilisers were calculated. The concentration of the stock solutions could be calculated from these extinction coefficients. Surface tension measurements over 30 minutes were carried out in Attension Theta Optical Tensiometer with a variety of dilutions (of stock solution) at room temperature. The mean value of surface tension in 30 minutes was calculated and used as the surface tension measurement of stabilisers.

2.6 Graphene dispersion preparation

Varying quantities (concentration from 2 to 8 mg mL^{-1}) of pyrene stabiliser were added in 6.0 mL deionised (DI) water, and then the mixture was heated to 80-90 ºC and stirred for 10 minutes to obtain a dispersion of stabiliser. The dispersion was tip sonicated (tip depth ~2 cm) for 20 minutes to ensure the dispersion is as homogenous as possible. A Misonix Sonicator 3000 was used for sonication at an output voltage of 24 W at room temperature. Graphite flakes were then added to the stabiliser dispersion and further tip sonicated for 1 h at an

output voltage of 9 W at room temperature. An ice-water bath was used in order to maintain the room temperature atmosphere of the sonication vessel. The graphite/graphene dispersion was then centrifuged (Eppendorf 5418 centrifuge) at 5000 rpm for 1 h to remove unexfoliated graphite flakes, and the supernatant was collected for further analysis. The whole synthesis process was repeated 5 times for each concentration.

The investigation of the stabilisers' concentration was based on the studies completed by Parviz *et al*[55]. The initial concentration of stabilisers was varied from 2.0 to 8.0 mg mL^{-1}. The ratio of the initial concentration of expanded graphite to initial concentration of stabiliser was 1:30 in order to give the best performance of exfoliation.

2.7 Characterisation of graphene dispersions

The concentration of graphene dispersion was determined by UV-Vis absorbance of diluted dispersion (using 1000 µL pipet) at 660 nm *via* Beer-Lambert law using the determined extinction coefficient (ε) of these graphene dispersions. For different stabilisers-base dispersions, different extinction coefficient values were used.

The determination of the ε value was based on the studies completed by Lotya *et al*[48]. Dispersion of stabiliser of concentration 3 mg mL^{-1} was prepared in DI water by heating to 80-90 ºC and stirred for 10 minutes. The mixture was then tip-sonicated for 20 minutes with an output power of 24 W at room temperature. Graphite powder was then added into the stabiliser dispersion and further tip-sonicated for 1 h at an output of 9W at room temperature. Three graphene-stabiliser dispersions were produced and then combined for analysing the UV-Vis absorbance. The absorbance of dispersions with a variety of dilution at 660 nm was measured, and then a Beer-Lambert plot was constructed. A pre-weighed polytetrafluoroethlene filter paper with a pore size of 0.022 µm was used for vacuum filtration of graphene dispersions. The mass of the filter paper before and after filtration was

measured and used to determine the gravimetric concentration of graphene dispersion. For two different stabilisers, two extinction coefficient values were determined. After the calculation, the initial concentration of graphene dispersant, whose stabiliser is Sodium 4-(pyren-1-yl)butane-1-sulphonate was 1.01 mg mL^{-1} demonstrating an ε value of 2500 mL mg^{-1} m^{-1}. For the Py-SO_3Na exfoliated graphene dispersion, the initial concentration was 0.41 mg mL^{-1} demonstrating a ε value of 1200 mL mg^{-1} m^{-1}.

2.8 Inkjet-printing conductive pattern of graphene dispersion

A piezoelectric Dimatix DMP-2800 (Fujifilm. Inc., USA) was used with a 10 pL cartridge (DMC -11610) in order to perform inkjet printing. The nozzle plate contains a set of 16 nozzles (diameter of each nozzle 21 µm) 254 µm apart in a single row. The print head height was set at 0.25 mm and the platen temperature was room temperature. The drop spacing is 20 µm, and a 27 V voltage was used on PEL paper. Graphene dispersion samples of both stabilisers Py-SASS (C_G ~ 0.4 mg mL^{-1}) and Py-C_4-SASS (C_G ~ 0.8 mg mL^{-1}) were used to print.

2.9 Measurement of sheet resistance

Two 1 × 1 cm^2 patterns were printed in 5 layers and 15 layers with conductive graphene ink on PEL paper in order to optimise the electrical conductivity in terms of sheet resistance of the printed patterns. Jandel four-point probe system (Jandel Engineering Ltd, Leighton UK) was used to measure the sheet resistance of the conductive pattern. The measurement was taken over 3 points and multiplied by a correction factor of 4.53, and it was averaged to get the result.

3. Result and Discussion

3.1 Computational study of stabilisers

As mentioned in section 1.6, our designed stabiliser is a pyrene sulfonic acid salt with a butyl spacer inserted between the pyrene aromatic unit and sulfonic acid salt. Since it is believed that a flexible spacer between the aromatic core and hydrophilic unit could enhance the performance of exfoliation. In order to evaluate the molecular design strategy, our collaborator Dr Flor Siperstein *et al*[60] at the University of Manchester performed the computational molecular dynamic simulations to calculate the potential mean force (PMF).

These simulations investigated the free energy of the adsorption process of stabilisers at various distance from a graphene surface in an aqueous medium. In the computational simulation cell (3.68 nm ×3.83 nm ×5 nm), the graphene sheet was placed in the x-y plane at z = 0. In addition, to simulate an infinite graphene sheet environment, periodic boundary conditions were used. The PMF curves of two stabilisers are shown in **Fig. 9**.

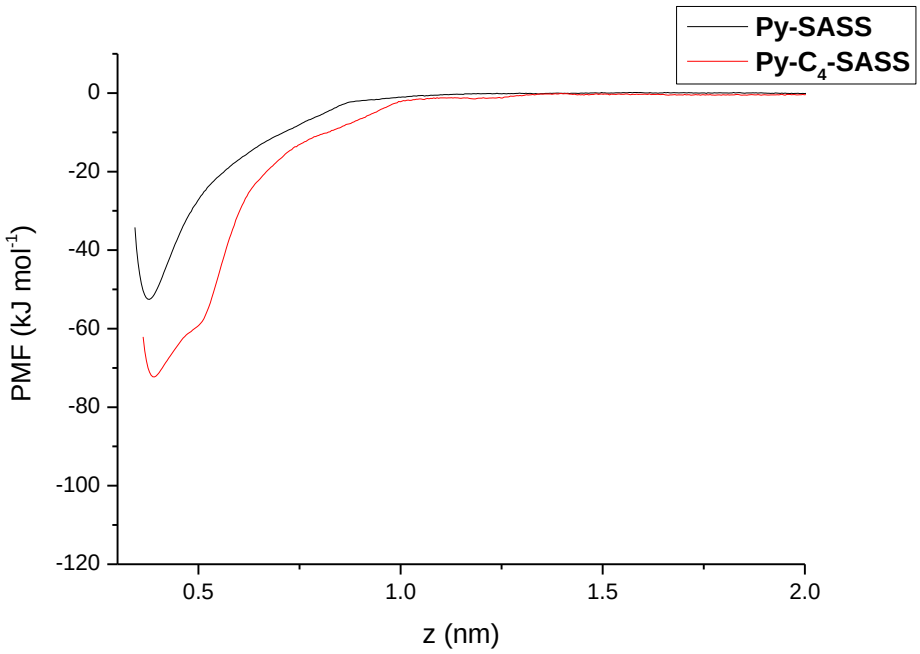

Figure 9: The PMF curves of two stabilisers

From the PMF curves, it shows when the stabilisers approach the graphene surface; the free energy decreases to a minimum value and then increases sharply. However, the minimum free energy of designed stabiliser Py-C_4-SASS is smaller than the stabiliser Py-SASS. **Table 1** summarises the exact value of the minimum adsorption free energy of each stabilisers and its associated distance from the graphene surface of graphene along the z-axis.

Chemical Structure	Adsorption free energy (kJ mol $^{-1}$)	z (nm)
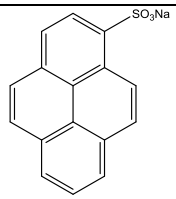 Py-SASS	-52.5 ± 0.2	0.38
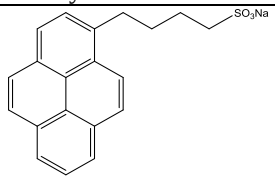 Py-C_4-SASS	-72.3± 0.8	0.39

Table 1: Investigation of Adsorption Free Energy of two stabilisers and the distance from the graphene sheet (z)

The results from both **Fig.9** and **Table 1**, suggest that the designed stabiliser Py-C_4-SASS has a stronger interaction with the graphene surface. This is because the longer butyl spacer decreases the steric effect among the sulfonic acid groups of stabiliser.

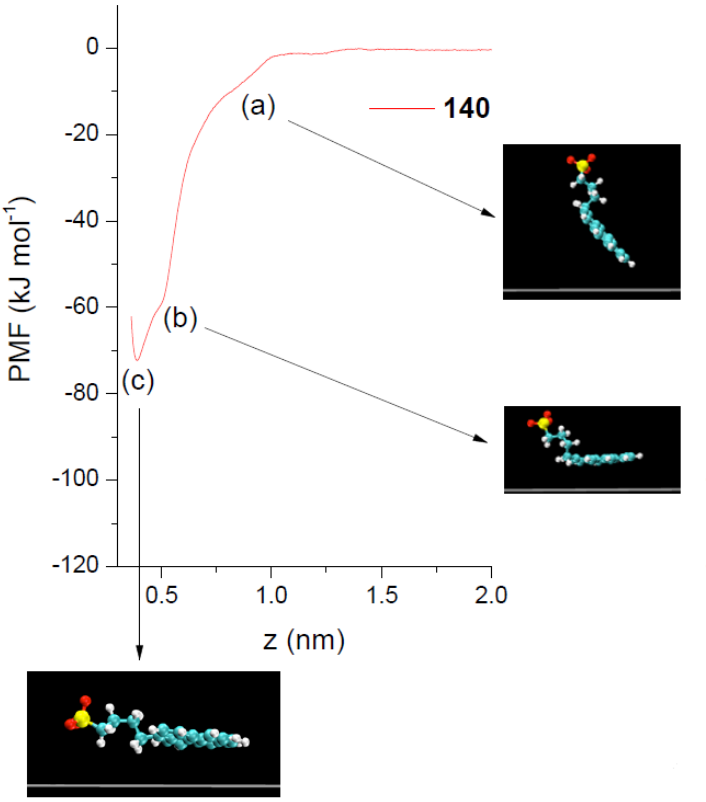

Figure 10: Calculated PMF curves of Py-C4-SASS with snapshots of the stabiliser molecule at various stages of interaction

Snapshots at different states of the molecular adsorption of Py-C_4-SASS were taken in order to have an insight into the mechanism of the stabiliser adsorbing onto the graphene basal plane. (**Fig. 10**) It is shown that, at stage (b), the pyrene core of the stabiliser and the graphene surface has reached the maximum π-π interaction state, and also at this stage, the sulfonic acid group is pointing away from the surface. Initially, it was expected that the sulfonic acid group would always pointing into the water medium and keep far away from the graphene surface. However in fact, it was observed in the simulation that the butyl chain also collapsed and interacted with the graphene surface, which finally resulted in a minimum state with sulfonic group far closer to the surface (stage (c)).

It is suggested that in the simulation, an installation of a butyl spacer can increase the interaction between the stabiliser and graphene surface, but it is important to note there is a significant drawback of these simulations. The computational simulation only measured the

interaction of a single stabiliser and single infinite graphene sheet. Therefore it does not factor in practical implications such as if the stabiliser became too insoluble in water to stabilise graphene sheets effectively. Furthermore, it was predicted that insertion of the butyl spacer could enhance the performance of the stabiliser not only because the charge from the graphene could be separated, but also the steric effect among sulfonic groups could be relieved when multiple stabilisers interact with the same graphene sheet. Using only one stabiliser is also fail to investigate the later prediction.

3.2 Synthesis of novel stabiliser-Py-C_4-SASS

Scheme 1 shows a three step route of synthesising Py-C_4-SASS stabiliser with a 6.7% overall yield. The detailed synthesis procedure can be found in section 4.1. The chemical structure has been verified by ^{1}H NMR, HRMS, IR and elemental analysis. It was designed for direct comparison with the commonly used commercially available stabiliser 1-pyrenesulfonic acid sodium salt (Py-SASS). It was hopped that inserting a more flexible butyl spacer could further ensure the hydrophilic unit and aromatic core could function more independently, so the performance of the stabiliser for exfoliating graphene would be enhanced in terms of final concentration of the dispersion. Owing to the insertion of a non-polar butyl chain, the solubility of stabiliser Py-C_4-SASS in water is decreased as its maximum concentration at room temperature is 1.94×10^{-3} mol L^{-1}, while the maximum concentration of stabiliser Py-SASS is 6.25×10^{-1} mol L^{-1}.

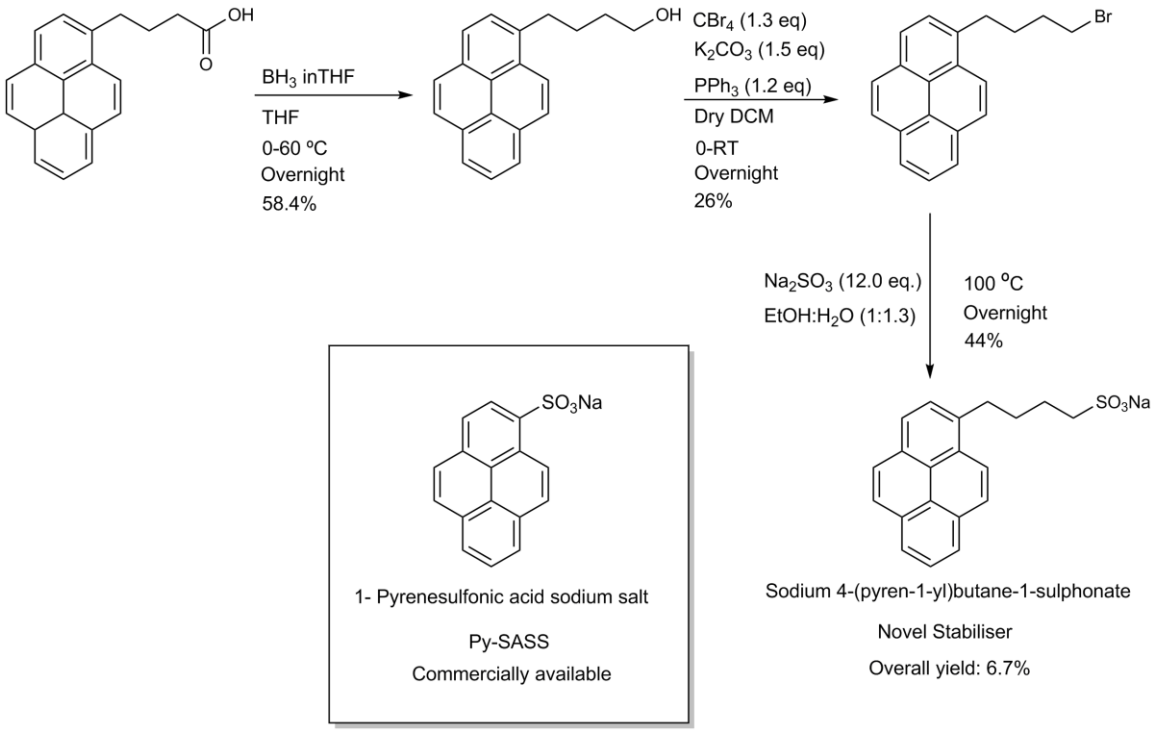

Scheme 1: Synthesis route of Sodium 4-(pyren-1-yl)butane-1-sulphonate and the comparison of 1-Pyrenesulfonic acid sodium salt (Py-SASS commercially available)

3.3 Surface tension comparison of two stabilisers

In the experiment, it was observed that the stabiliser Py-C_4-SASS may have higher viscosity than Py-SASS, after the stabiliser dispersion is shaken vigorously, some bubbles will appear, and this phenomenon is not be seen in Py-SASS solution. Therefore, we presume that with an insertion of butyl spacer, the designed stabiliser might be behaving more like a surfactant.

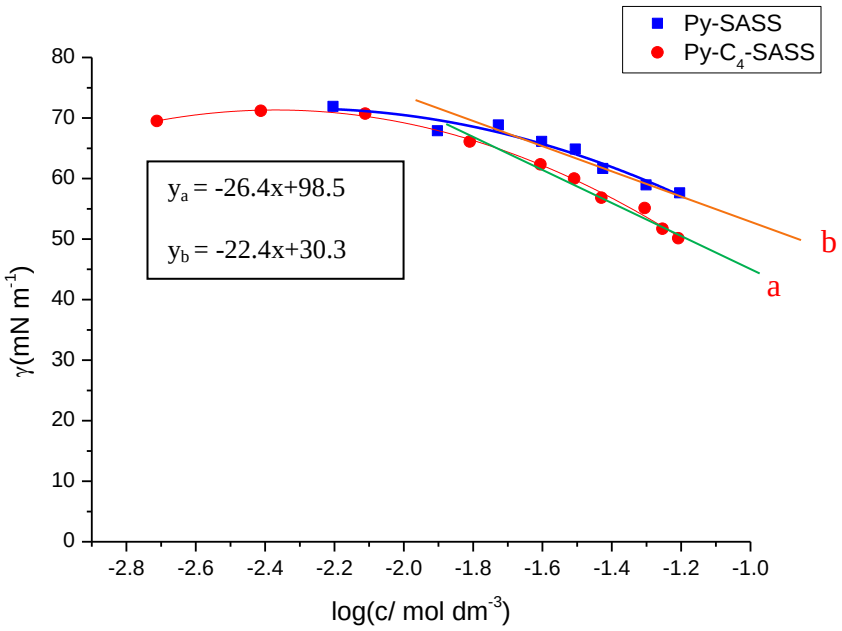

Figure 11: The surface tension comparison of two stabilisers (orange: tangent line for Py-SASS; green: tangent line for Py-C_4-SASS)

To confirm this assumption, the surface tension of the two stabilisers at various concentrations was measured. According to **Fig. 11**, although it could lower down the surface tension of water more effectively than Py-SASS, critical micelle concentration has not been found in this experiment. Hence, Py-C_4-SASS is not a surfactant. However, the partial surface tension curve could be used to calculate the surface excess (Γ_2) in order to predict the surface area (A_{min}) of the stabilisers, and to evaluate their ability of occupying a surface.

$$\Gamma_2 = -\frac{1}{2.303RT}\left(\frac{d\gamma}{d\log_{10} C}\right) \quad \text{.....Equation 1}$$

$$A_{min}(in\ nm^2) = \frac{1\times10^{18}}{N_A\Gamma_2} \quad \text{.....Equation 2}$$

Where N_A is Avogadro number, Γ_2 is surface excess in mol m^{-2}.

According to **Fig. 10,** and **Eqn. 1,**

$$\Gamma_{2,Py-SSAS} = -\frac{-26.4\times10^{-3}}{2.303\times8.314\times298} = 4.6\times10^{-6}\ mol\ m^{-2}$$

$$A_{\min(Py-C_4-SSAS)} = \frac{1 \times 10^{18}}{6.022 \times 10^{23} \times 4.6 \times 10^{-6}} = 0.36\ nm^2$$

and

$$\Gamma_{2,Py-SSAS} = -\frac{-22.4 \times 10^{-3}}{2.303 \times 8.314 \times 298} = 3.9 \times 10^{-6}\ mol\ m^{-2}$$

$$A_{\min(Py-C_4-SSAS)} = \frac{1 \times 10^{18}}{6.022 \times 10^{23} \times 3.9 \times 10^{-6}} = 0.43\ nm^2$$

The gradient $\left(\frac{d\gamma}{d\log_{10} C}\right)$ of the line for Py-C_4-SASS is about ~ -26.4 whereas the gradient of the line for Py-SASS is about ~ -22.4; therefore, the gradient for the designed stabiliser is slightly higher the commercially available stabiliser. According to **Eqn. 1**, the surface excess of stabiliser Py-C_4-SASS is ~4.6×10^{-6} mol m^2, while the surface excess of stabiliser Py-SASS is ~ 3.9×10^{-6} mol m^2. Thus, the minimum surface area of stabiliser Py-C_4-SASS is ~0.36 nm^2 whereas the minimum surface area of stabiliser Py-SASS is 0.43 nm^2. Therefore the minimum surface area of stabiliser Py-C_4-SASS is slightly smaller than stabiliser Py-SASS.

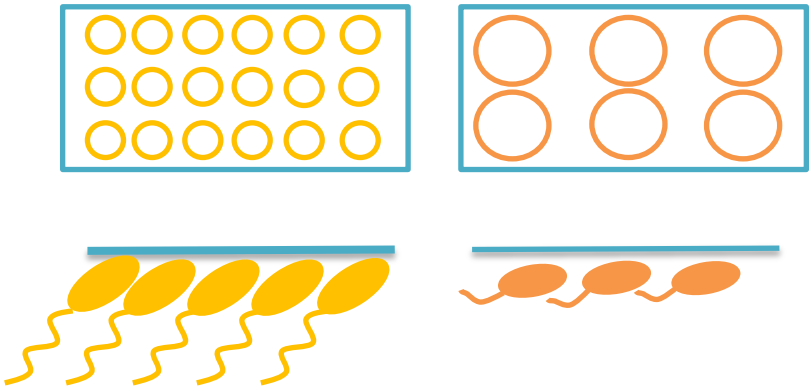

Figure 12: Occupancy difference in water for molecule with different surface area

As shown in **Fig. 12**, when the total surface area of the surface is the same, the molecule with the smaller surface area, more of them can occupy more positions on the surface. As mentioned in section 3.1, when stabiliser Py-C_4-SASS interacts with the graphene sheet

surface, the butyl spacer will lie down to participate in the interaction with graphene as well, while the tensiometry result shows the hydrophilic tail of stabilisers might prefer pointing into water when it get close to the water surface. The computational simulation and tensiometry results seem to contradictory with each other. However, the surface tension measurement only shows stabiliser Py-C_4-SASS to occupy a smaller surface area in water, yet how the surface area occupancy status with the presence of graphene is remain unknown. Moreover, the simulation PMF result only simulates the interaction and one stabiliser with one graphene infinite sheet, as tensiometry measurement show the results from multiple stabilisers interacting with water. Therefore, it is hard to draw a conclusion from combining these two results, since they actually fail to agree with each other at this point because the variables in the experiment are out of control. Some further simulation work is needed in order to study the mechanism of how multiple stabilisers would interact with one graphene sheet.

3.4 Stabiliser assisted liquid phase graphene exfoliation

3.4-1 Comparison of the exfoliation ability of stabilisers for graphene

The performance of the stabilisers Py-C_4-SASS and Py-SASS are compared with respect to their ability to create graphene dispersions in aqueous liquid phase exfoliation. Based on the work of Parviz *et al*[55], owing to the weak solubility in water the two stabilisers were tip sonicated first to ensure the dispersion was homogeneous, and then the stabiliser dispersion was further tip sonicated in the presence of graphite flakes. The samples were then centrifuged for 1 hour at 5000 rpm to remove the excess unexfoliated graphite flake. After centrifugation, the supernatant was kept for further analysis. Diluted samples were analysed by UV-vis spectroscopy and their absorbance at 660 nm used to determine the degree of exfoliation of graphite.

To directly compare the exfoliations yield, the UV-vis absorbance of the graphene dispersions was measured. According to the Beer-Lambert law, A= εcl (ε is extinction coefficient, c is concentration and l is path length of the cuvette), concentration can be derived, c = A/εl. The extinction coefficient ε is a constant which is independent to the concentration of graphene, and its value should be the same for all graphene dispersion. Therefore, when ε is unknown, absorbance divided by path length (A/l) could be used as the feature to compare the degree of exfoliation.

In the work of Parviz *et al*[55], the stabiliser Py-SASS was sonicated in water at concentrations from 1 mg mL^{-1} to 7 mg mL^{-1}. The ratio of initial concentration of expanded graphite ($C_{EG,\,i}$) to initial concentration of stabilisers (C_s) was 30. A similar experiment method was repeated in this project. Both stabilisers Py-SASS and Py-C_4-SASS were sonicated in aqueous solution at concentration from 2 mg mL^{-1} to 8 mg mL^{-1}, and the ratio of initial graphite concentration ($C_{G,i}$) to initial stabiliser concentration (C_s) was 30. For each stabiliser concentration, the experiments were repeated 5 times. UV-vis absorbance analysis at 660 nm of post-centrifuged dispersions allowed the construction of **Fig. 13**.

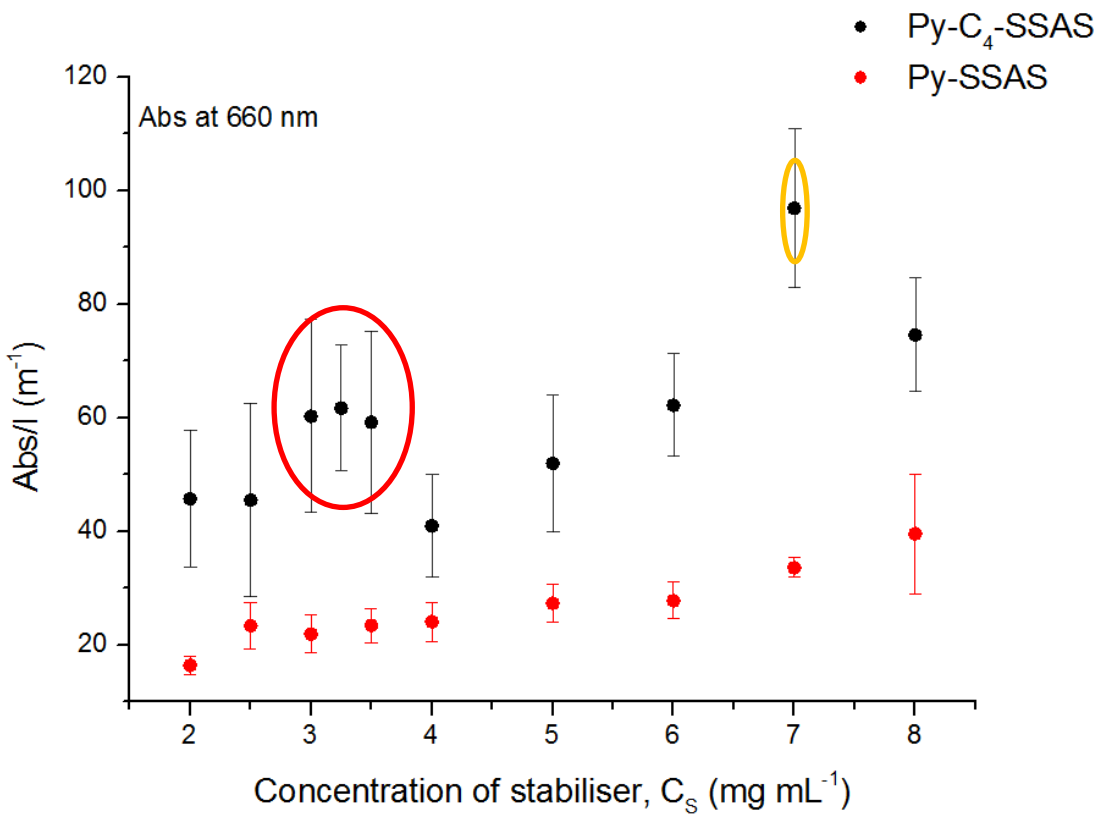

Figure 13: The comparison of exfoliate ability to graphene for two stabilisers (circle shown the two optimum performance of stabiliser)

In the work carried out by Parviz *et al*[55], when the concentration of stabiliser Py-SASS was 3 mg mL^{-1}, the performance was found to be the best, and gave the concentration of graphene dispersion to ~ 0.8 - 1 mg mL^{-1}. However, as illustrated in **Fig.13**, we do not observe the same trend, the concentration of the graphene dispersions changes very little as the stabiliser concentration is increased. Most notably, almost all $A/l_{(G,\ Py\text{-}C4\text{-}SASS)}$ values are twice higher than $A/l_{(G,\ Py\text{-}SASS)}$, showing that stabiliser Py-C_4-SASS has stronger stabilisation ability than stabiliser Py-SASS. Despite the fact that Py-C_4-SASS has poorer solubility in water than Py-SASS, it is still showing a better capability of stabilising graphene. It is notable in the result that even though the designed stabiliser is behaving better than the commercially available stabiliser, the error in Py-C_4-SASS exfoliated graphene dispersion is much larger (**Fig.13**).

Owing to the low solubility of Py-C_4-SASS, even though it has been pre-sonicated in water to ensure it is as homogeneous as possible, it still could not dissolve or disperse evenly in the water, so it is not able to perform continuously over five experiments.

Moreover, looking closely at the behaviour of Py-C_4-SASS (black dots in **Fig.13**), there are two points which break in the trend. The A/l value of graphene dispersion increase as the concentration of stabiliser increases, and it reaches the first optimum value (~62 m^{-1}) when $C_{(s.\ Py\text{-}C4\text{-}SASS)}$ is 3.25 mg mL^{-1}, then it starts to decreases and reach the lowest value when $C_{(s.\ Py\text{-}C4\text{-}SASS)}$ is 4 mg mL^{-1}. However, after the lowest valley of the trend line, the A/l value starts to increase again while the $C_{(s.\ Py\text{-}C4\text{-}SASS)}$ further increase and then reaches as maximum value (~ 95 m^{-1}), before finally decreasing back when $C_{(s.\ Py\text{-}C4\text{-}SASS)}$ increases to 8 mg mL^{-1}.

It was observed in the experiment, when the concentration of stabiliser Py-C4-SASS is below 4 mg mL^{-1}, the stabiliser could dissolve in water under high temperature (90 ºC). Although the solution/dispersion is not stable enough to remain dissolved after cooling down to room temperature (it becomes opaque), the status of the whole system is still relatively stable, as there is not appearance of aggregation or precipitation. Therefore, in the result shown in **Fig. 13**, at 3.75 mg mL^{-1}, it is likely that when the stabiliser forms a stable dispersion in water (where concentration is smaller than C_{min} (~4 mg mL^{-1})), the graphene flakes need more stabilisers to cover their surface, otherwise they will start to aggregate. Hence, when $C_s < C_{min}$, more stabilisers is needed to stabilise the graphene.

Nevertheless, when the saturation point (C_{min}) of stabiliser in water is passed, the stabiliser starts to self-aggregate, and tends to have π-π interactions with itself rather than the graphene sheet. That might be the reason why the A/l value decreases after the first maximum value where $C_{(s.\ Py\text{-}C4\text{-}SASS)}$ is 3.25 mg mL^{-1} (**Fig. 13**). Once $C_s > C_{min}$, the mechanism becomes a more kinetic process. Therefore, as more stabiliser molecules are used, the more the graphene could be stabilised in water, and when it gets to a point where water can no longer maintain a

stable dispersion with stabiliser (when $C_{(s.\ Py\text{-}C4\text{-}SASS)}$ = 8 mg mL^{-1}), the A/l value decreases again. However, the mechanism behind this second bump behaviour remains unclear.

3.4-2 Extinction coefficient measurement

To continue measuring the concentration of graphene dispersion by UV-Vis, an extinction coefficient (ε) is needed for these dispersion with Py-C_4-SASS and Py-SASS stabiliser. **Scheme 2** is the flow diagram for the method of measuring the extinction coefficient (ε).

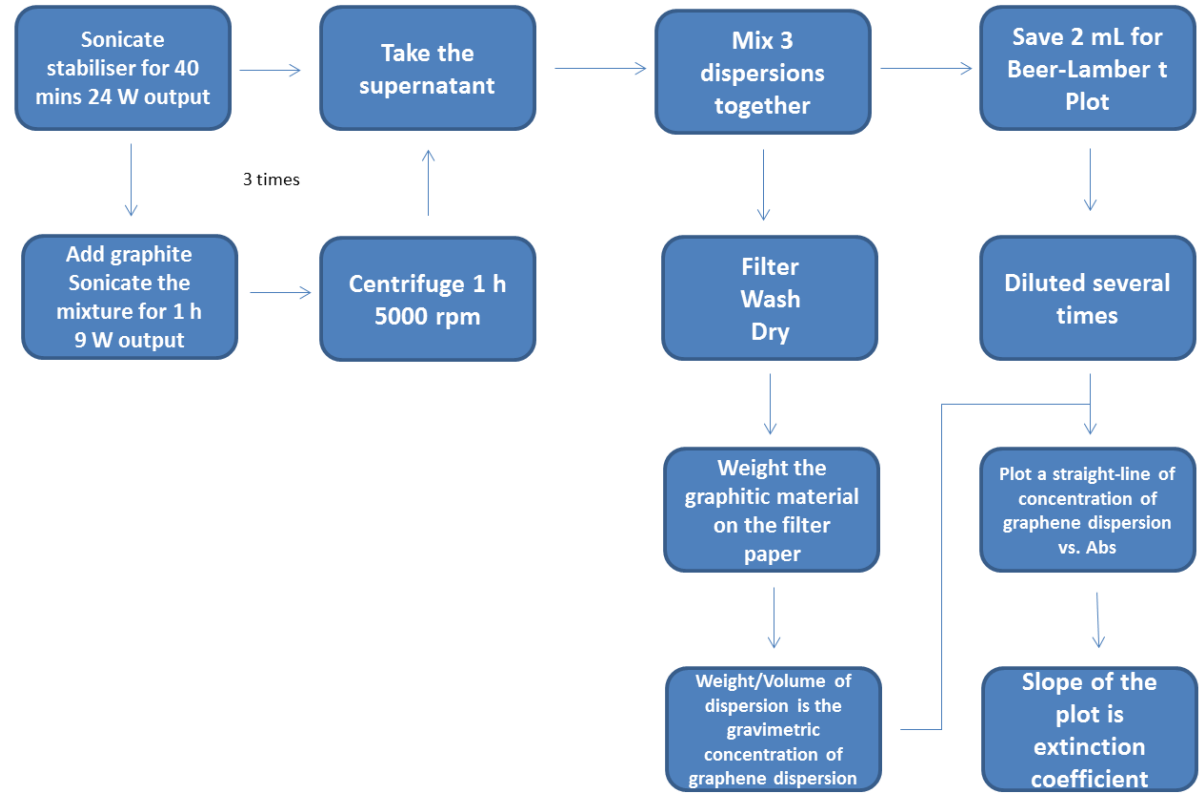

Scheme 2: The flow diagram of measuring the extinction coefficient of graphene dispersions

As shown in **Scheme 2**, to determine the extinction coefficient, a Beer-Lambert plot and the gravimetric graphene concentration for the respective dispersions is needed. For making Beer-Lambert plot, the absorbance at 660 nm in the UV-Vis spectrum of a series of diluted graphene dispersion with graphene initial concentration ($C_{G,\ i}$ = 90 mg mL^{-1}), stabilisers

concentration, C_s = 3 mg mL^{-1}) was measured. After that, the un-diluted dispersion was filtered through a pre-weighed porous filter paper, and after drying the filter paper, the mass of graphitic material was measured using a micro-balance. With the volume of dispersion and the mass of graphitic material known, the gravimetric concentration (c) of graphene dispersion could be calculated. With the gravimetric concentration (c), the extinction coefficient (ε) could be calculated. (**Eqn. 4**)

$A = \varepsilon c l$ ……..Equation 3

$\frac{A}{l} = \varepsilon c$ ……...Equation 4

In the Beer-Lambert plot (**Fig. 14)**, the absorbance at 660 nm divided by the path length (A/l) was plotted against a series concentration of graphene dispersion. The gradient of these plots therefore give the extinction coefficient (ε) for the respective dispersion (**Eqn.4**).

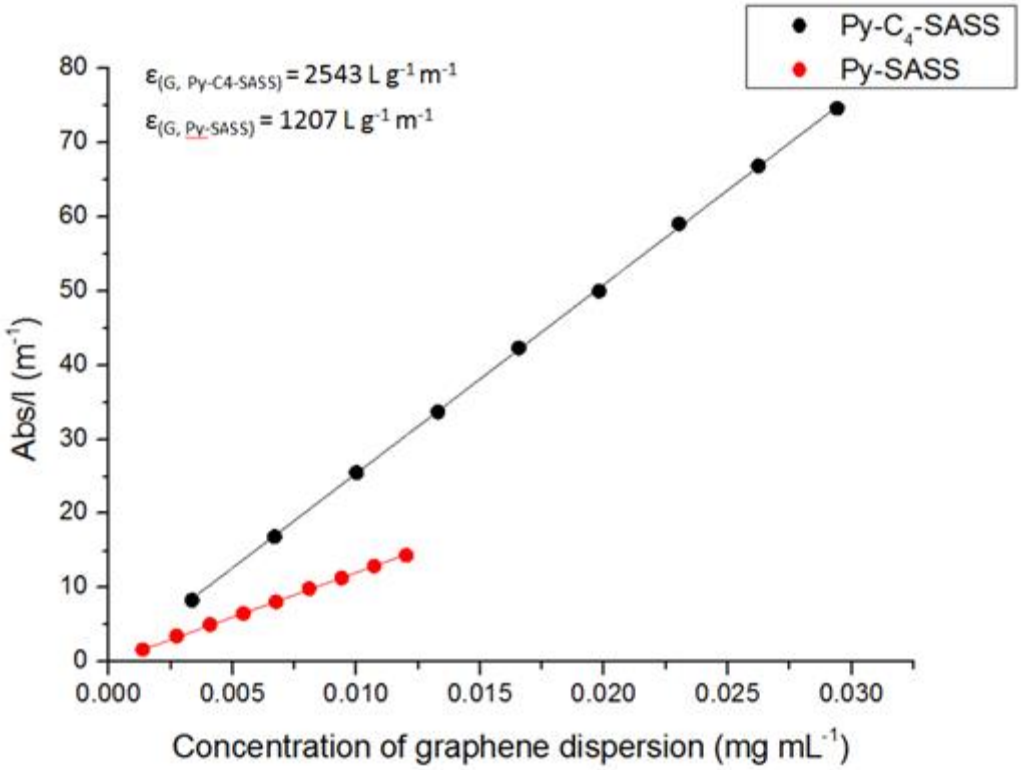

Figure 14: Beer-Lambert plots of absorbance *vs.* concentration of graphene dispersion using Py-C_4-SASS and Py-SASS stabilisers to measure the extinction coefficient.

It is known from the literature that the extinction coefficient of graphene dispersion is variable (from ~ 1390 L g^{-1} m^{-1} to 6600 L g^{-1} m^{-1}) even when identical experimental condition is used.[32] As shown in **Fig. 14**, similarly to the literature, despite maintaining the same experimental conditions, two different extinction coefficient values of $\varepsilon_{(G,\ Py\text{-}C4\text{-}SASS)}$ = 2543 L g^{-1} m^{-1}, and $\varepsilon_{(G,\ Py\text{-}SASS)}$ = 1207 L g^{-1} m^{-1} were produced. This disparity in the extinction coefficient might be because liquid phase exfoliated graphene has variation in lateral flake size and thickness distribution which could affect its absorbance in UV-Vis spectroscopy.[32]

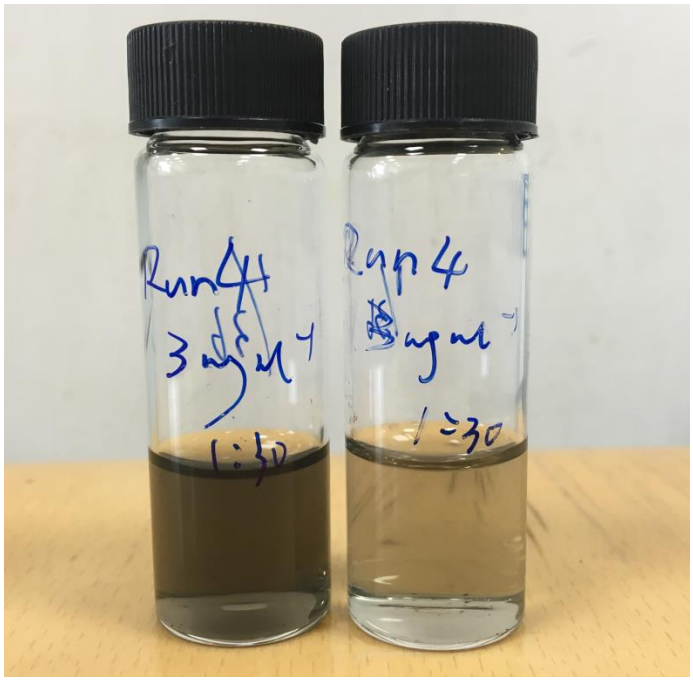

Figure 15: Graphene dispersion at same dilution (diluted 36 times) when the concentration of the stabiliser at 3 mg mL^{-1} (left: Py-C_4-SASS; right: Py-SASS)

Since the value of the extinction coefficient is unclear, it is unsuitable to use in the calculation of the concentration and exfoliation yield for all graphene dispersions. However, as shown in **Fig. 15** the graphene dispersion with Py-C_4-SASS is visibly darker than the dispersion with Py-SASS suggesting a higher graphene concentration. Additionally, the gravimetric concentration of graphene produced by using two different stabiliser at 3 mg mL^{-1} also confirms that designed stabiliser Py-C_4-SASS is better at stabilising graphene than Py-SASS, as the $C_{(G,\ Py\text{-}C4\text{-}SASS)}$ is 1.01 mg mL^{-1} while $C_{(G,\ Py\text{-}SASS)}$ is 0.41 mg mL^{-1}.

3.5 Characterisation of graphene flake quality

It has been shown (section 3.4-1) that the novel stabiliser (Py-C_4-SASS) for graphene exfoliation works well at a concentration of ~3 mg mL^{-1}. Therefore, to directly compare the performance of the two stabilisers, the two graphene dispersions at this stabiliser concentration were selected as the samples to analyse. Here, Raman spectroscopy, SEM and

AFM were used to characterise the exfoliated graphene sheets. Both graphene samples that were exfoliated with the assistance of different stabilisers were prepared by pipetting two drops of diluted graphene dispersion onto a 290 nm SiO_2|Si substrate and then spin coated at 1200 rpm for 5 minutes.

3.5-1 Raman Spectroscopy

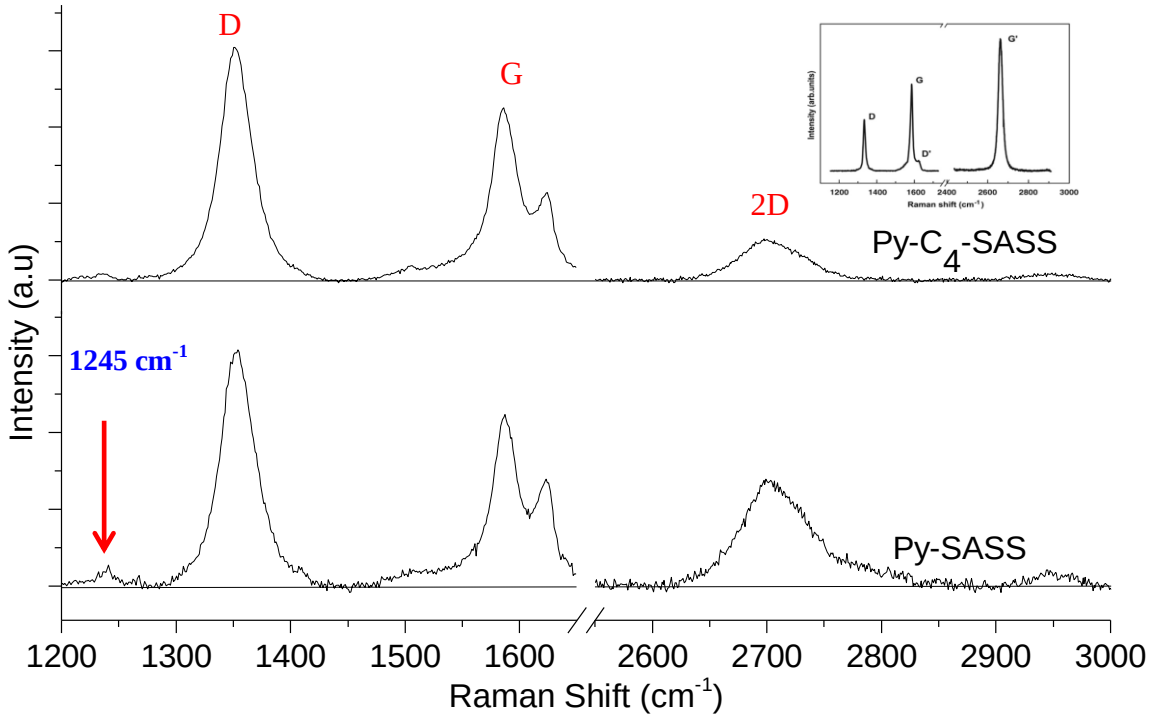

Figure 16: Raman spectroscopy of graphene dispersion by using the designed stabiliser (Py-C4-SASS). (Inset) Raman spectrum of a graphene edge (modified from ref. 31)

Raman spectroscopy was performed on graphene flakes deposited on silicon substrate. **Fig. 16** is the Raman spectra measured on the flakes (exfoliated separately by two different stabilisers) with excitation at 514 nm. The G band is at around 1580 cm^{-1}, the 2D band is at around 2700 cm^{-1} and the D band is at around 1350 cm^{-1}.

Also, compared to the typical Raman spectrum of a graphene edge (**Fig. 16.**inset), it could be predicted that an intense D band is caused by both edge effects and defects from the graphene flakes. Since the excitation beam spot size of Raman is ~1 μm, which is larger than some of the flakes on the substrate. However, the presence of this feature does not mean the defects of

graphene could be ruled out as the edge spectrum of pristine graphene above shows a much smaller D band.

It is obvious that more noise is shown in the Raman spectrum for Py-SASS assisted exfoliated graphene. This was due to the difficulty in acquiring a clean Raman spectrum with the presence of stabiliser Py-SASS owing to the strong fluorescence background from the pyrene moiety.[57, 64] However, the designed stabiliser Py-C_4-SASS did not have this issue to the same degree; hence the higher intensity of Raman signal can be observed. A higher wavelength laser was used (633 nm) to try and reduce this noise but it only increased the noise and needed much longer acquisition times in order to get any signal. The excess is further shown by the small peak at ~1245 cm^{-1} that appears in the spectrum of Py-SASS assisted exfoliated graphene. According to the Raman spectroscopy study of pyrene crystals by Dreger *et al*[65], this small peak is attributed to the pyrene aggregates. Such a pyrene peak is less intense in the spectrum for the other graphene.

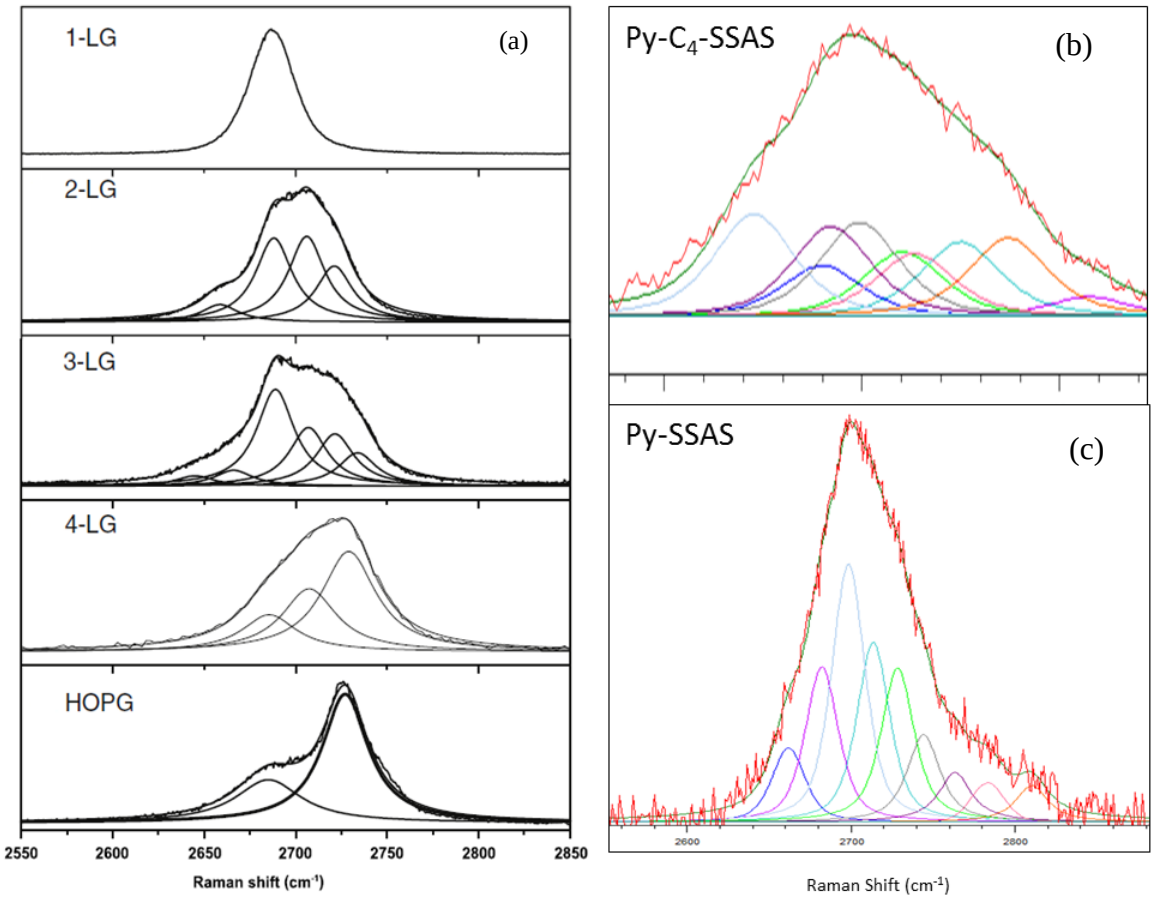

Figure 17: (a) The measure 2D Raman band from 1-LG to HOPG (adapted from ref. 31) (b) 2D Raman band (Py-C_4-SASS) (c) 2D Raman Band (Py-SASS)

Peak fitting was performed on the 2D band, the most informative band from graphene Raman spectroscopy when analysing the number of graphene layers. Compared to the literature **Fig. 17(a)**, the peak fitting of the 2D band from our sample is more upshifted than the 2D band of single layer graphene **Fig 17 (c)**. Furthermore, the splitting pattern of these bands is more like a combination of double-layer and three-layer graphene, by comparison to the literature. In summary from Raman spectroscopy, both kinds of flakes on the substrate are almost few layers graphene, and yet AFM data is needed to further support this conclusion.

3.5-2 Scanning Electron Microscopy and flake size distribution

A SEM analysis of the graphene samples was conducted to further characterise the form of nanocarbon in the dispersion. The same samples used for Raman spectroscopy were used for SEM analysis.

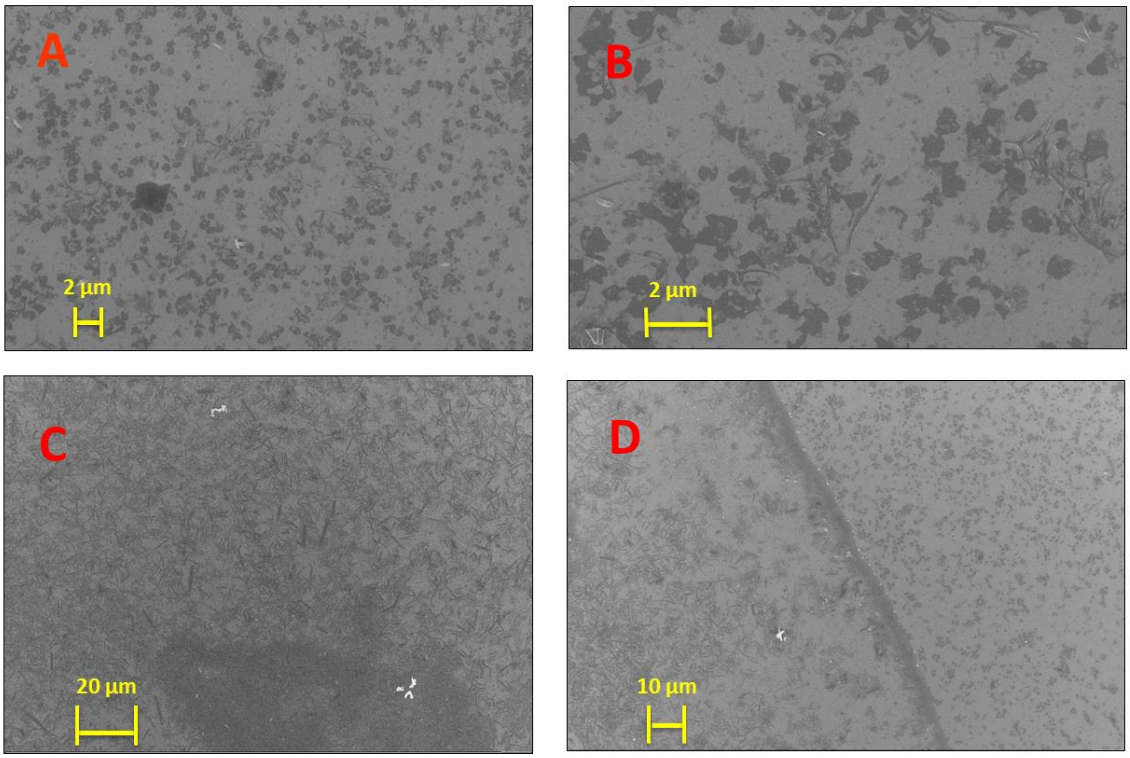

Figure 18: Selected SEM images of flakes prepared by Py-C_4-SASS assisted exfoliation of graphite. (A) & (B) An overall look of graphene flakes (C) Some rod shape material in the dispersion (D) Flake and rod appearing together with a clear line of separation

Fig. 18 shows some selected SEM images of graphene flakes which were exfoliated with the assistance of stabiliser Py-C_4-SASS. From images (A) and (B), many of the flakes had a diameter of ~0.4 µm. Most of the flake sizes are smaller than 1 µm, which agree with the large D band shown in the Raman spectra.

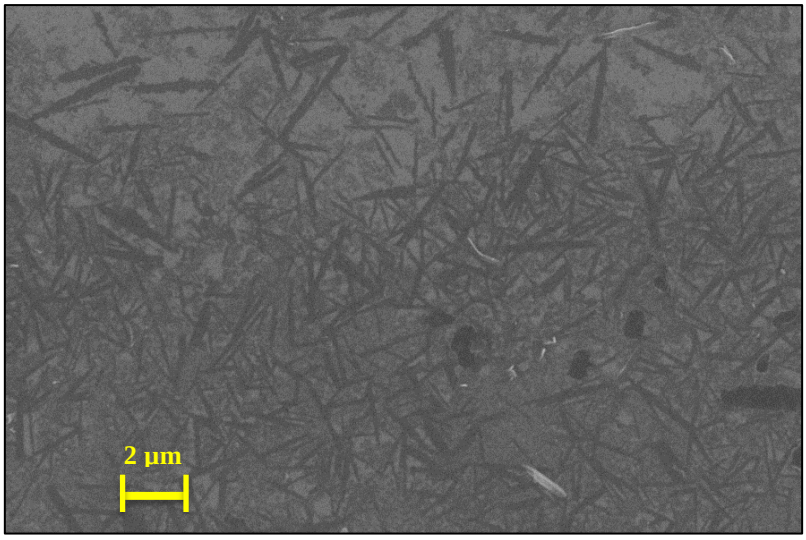

Figure 19: Magnified image of rod shape material

Fig. 18 (C) and Fig. 19 are images of some rod shaped crystalline material which appear on the substrate. From the magnified image **Fig. 19,** the type of this material is unable to be characterised yet. It could be excess stabiliser crystal or poor-exfoliated graphite. Raman analysis was attempted but there appeared to be a large amount of florescence and an increase in noise. Furthermore, the clear boundary between the rod shape material and graphene flakes in **Fig. 18 (D)** shows that the graphite is not evenly exfoliated in water. It is expected that all graphite cannot be exfoliated in the same way by using tip sonication, since it is a vigorous technique for exfoliation, whose power is hard to control although the same depth of tip (~ 2 cm) into water is maintained over every experiment. The degree of exfoliation for graphite depends on its distance to tip and the propagation of the sound waves through the water etc. In order to get a more homogeneous and larger size exfoliated graphene some gentler technique e.g. shear mixing might be a better choice.[66]

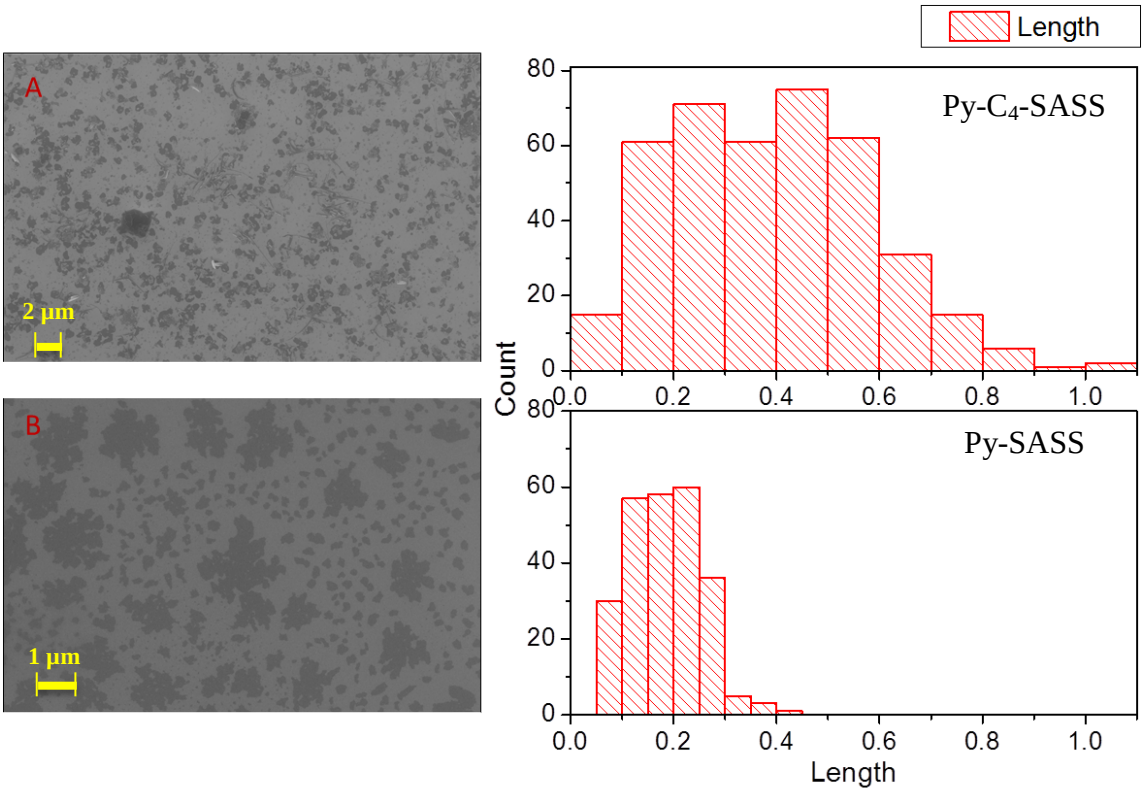

Figure 20: Flake size distributions of different stabiliser assisted exfoliated graphene by using left side SEM image

Fig. 20 shows the SEM images of graphene flakes which were exfoliated with the assistance of stabilisers and the flake size distribution from the SEM images. According to the distribution, the diameter of the flakes, which were exfoliated with assistance of stabiliser Py-SASS, are around 0.15 ~ 0.25 µm. In addition, there are some larger flakes ~2 µm in diameter, however these are not single graphene flakes, but aggregates formed by many smaller flakes. For the stabiliser Py-C_4-SASS exfoliated graphene flakes, the distribution shows the diameter of flakes are around 0.1 ~ 0.6 µm, slightly more polydisperse than the commercial stabiliser.

From both SEM images and flake size distribution of two dispersions, it is obvious that the Py-C_4-SASS assisted graphene dispersion has higher quality flakes than the Py-SASS

exfoliated one. Nevertheless, SEM cannot distinguish the numbers of layers in a graphene flake, thus AFM is needed to measure the height of the flakes.

3.5-3 Atomic Force Microscopy

An AFM analysis for the stabiliser Py-C_4-SASS assisted exfoliated graphene suspension at C_s = 3 mg mL^{-1} was done to further characterise the thickness of the graphene flakes deposited on the $Si|SiO_2$ substrate.

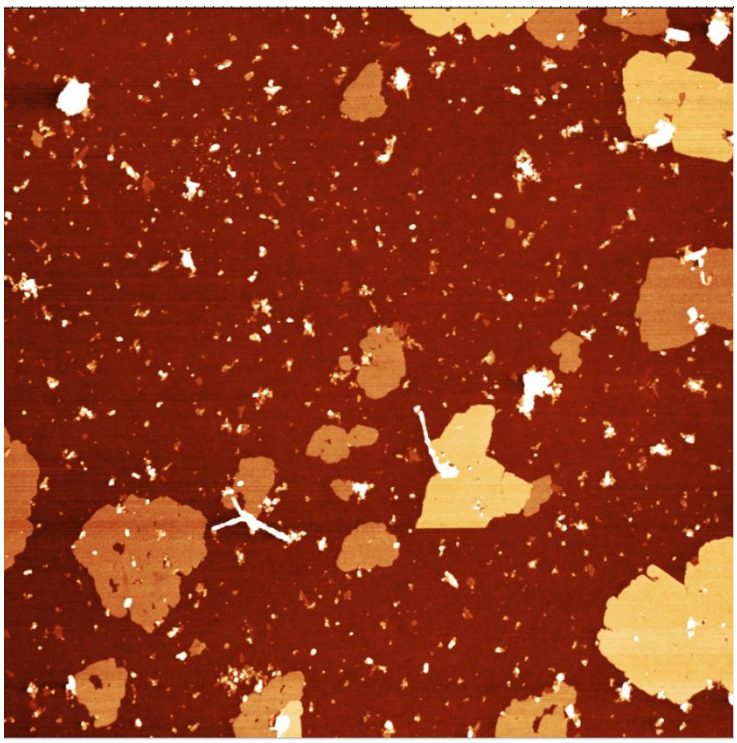

Figure 21: AFM images of the few-layer graphene flakes deposited on a $Si|SiO_2$ substrate

Fig. 21 is an atomic force microscopy (AFM) image with graphene flakes deposited on $Si|SiO_2$ substrate after graphene deposition. A number of large graphene flakes with an average lateral size of 2 µm can be found. A large number of smaller flakes with an average lateral size of 0.6 µm could be seen as well.

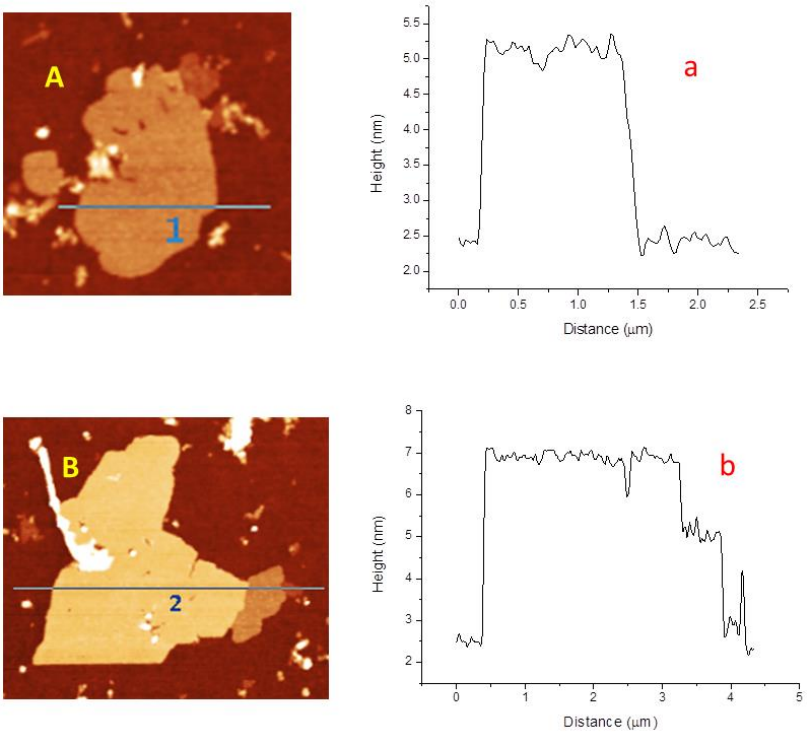

Figure 22: (A) & (B) Selected zoomed AFM images. (a) & (b) Height profiles for the corresponding to the line shown in the AFM images

Fig. 22 (a) & (b) shows the height of the flakes underneath the line in left hand side images. For the flake in **Fig. 22 (A)**, the height is ~3 nm, and the height is ~ 4.5 nm for the flake in **Fig. 22 (B)**. It is notable that the flake in **Fig. 22 (B)** looks like the aggregation of two graphene flakes since there is a drop down in height when the straight line goes to the right. It could be two graphene flakes stack together to get this ~ 4 nm height graphene. The lateral size of these two flakes is around 2 μm.

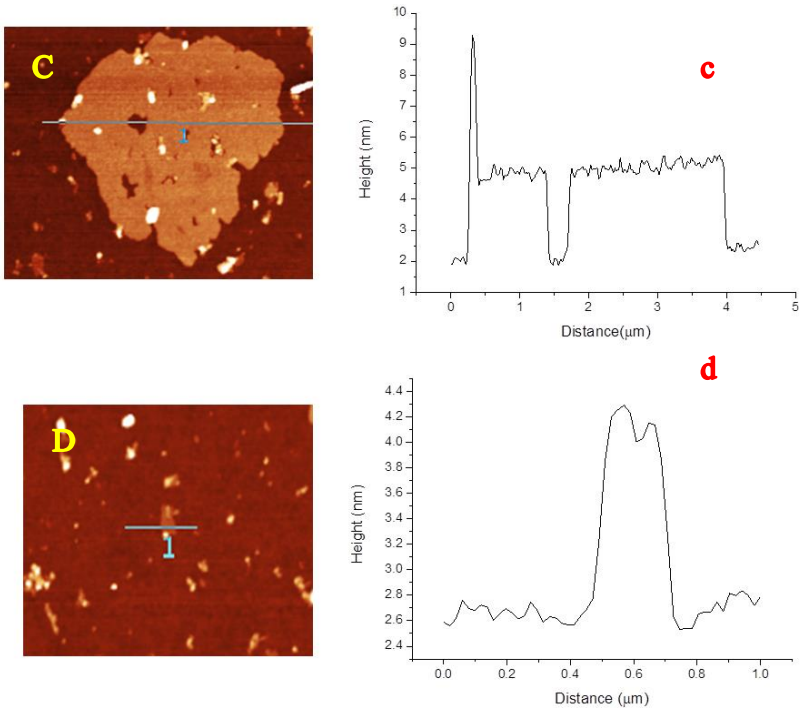

Figure 23: (C) & (D) Selected zoomed AFM images. (c) & (d) Height profiles for the corresponding to the line shown in the AFM images

Fig 23 (C) is another zoomed image of a graphene flake yet with thinner thickness, as **Fig. 23 (c)** shows the height of the flake is around 2 nm. Furthermore, it is obvious that there are some holes in the flake (a sharp drop down shown in the corresponding height profile as well), which is predictable since tip sonication is such a violent technique that some graphene flakes might be broken down during exfoliation. Some stabilisers aggregate on the graphene flake which gives the sharp increase in height, however the size of aggregation is around 0.1 μm, and the flake is not evenly covered by the stabilisers. **Fig. 23 (D)** is a very small graphene flake with lateral size around 0.5 μm, and its height is around 2 nm as well. From **Fig. 21** we could know that although with the presence of decent size graphene flakes, the majority lateral size of the graphene flakes deposited on the substrate is relatively small (~ 0.5 μm), which is in good agreement with the flake size distribution from the SEM images. Most importantly, the thickness analysis of graphene flakes shows the height of the majority of the

graphene flakes is around 2~4 nm, indicating that the majority of them are single and few layer graphene, which agrees with the Raman spectroscopy result that most of the graphene are few layer graphene (no more than 4 layers). However, with limited time, the AFM analysis of stabiliser Py-SASS assisted exfoliated graphene suspension cannot be done to give a more direct comparison.

3.6 Inkjet-printing

The inkjet printing is chosen because of a previously successful study using silver nanoparticle inks.[67] Therefore, we inkjet-printed our best performance samples to investigate the conductivity of our graphene dispersions.

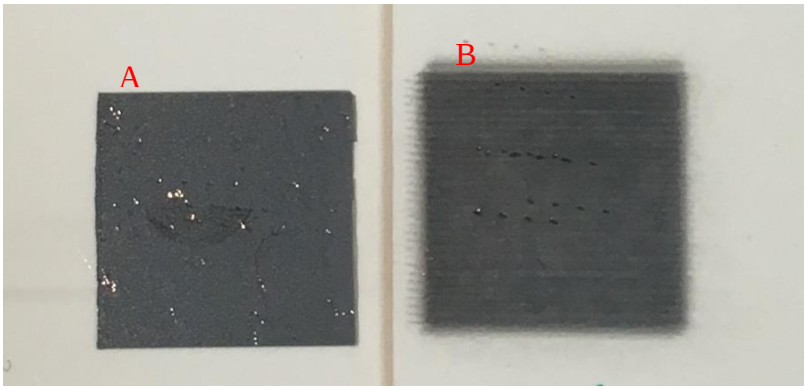

Figure 24: Inkjet printing pattern of two graphene stabilisers (A: Py-C4-SASS assisted (5 layers); B: Py-SASS assisted (15 layers))

Py-C_4-SASS (kΩ) Pattern A	Sheet resistance (kΩ/sq) (Correction factor: 4.32)	Py-SASS (kΩ) Pattern B	Sheet resistance (kΩ/sq) (Correction factor: 4.32)
19.95	86.18	26.86	116.04
19.42	83.89	42.24	182.48
18.80	81.22	45.61	197.04
Average	83.76	42.89	185.28
		Average	170.21

Table 2: Sheet resistance of graphene printed patterns

The graphene concentration ($C_{(G,\ Py\text{-}C_4\text{-}SASS)}$) of the printed ink of pattern A is ~0.8 mg mL^{-1}, whereas $C_{(G,\ Py\text{-}SASS)}$ of the printed ink of patter B is ~0.4 mg mL^{-1}. However, the surface of PEL paper is very rough and a few passes layers is very thin due to the low concentration of dispersions. Therefore, it was a challenge to measure the height of the patterns. Herein, we could only assume the height of the two patterns is same. According to the calculation in **Table 2**, the average sheet resistance of pattern A (Py-C_4-SASS assisted exfoliated graphene ink) is 83.76 kΩ/sq, whereas the average sheet resistance of pattern B (Py-SASS assisted exfoliated graphene ink) is 170.21k Ω/sq. With lower sheet resistance, the higher the conductivity of the pattern, hence the conductivity of pattern A is higher than pattern B. This should be attributed to the better stabilisation ability of the novel stabiliser Py-C_4-SASS which could produce higher concentration graphene dispersion with large lateral size and less damaged graphene flake. Additionally, it is believed the presence of residual stabiliser in the graphene dispersion will affect the performance of conductivity. Therefore, in order to further increase the conductivity of printed graphene pattern, the excess stabiliser residual in graphene ink needs to be removed. However, full characterisation (e.g. height of the patterns) and optimisation (e.g. remove residual stabiliser molecules) of these printed patterns are required for further insight.

4. Conclusion and Further work

4.1 Conclusion

In this project, a novel, scalable pyrene base stabiliser (Py-C_4-SASS) was synthesised for the liquid phase exfoliation of graphene in water and compared to a commercially available alternative (Py-SASS). Both stabilisers can produce stable graphene suspension in water, and the Raman spectroscopy shows that a relevant fraction of few layer graphene (≤ 4 layers) was obtained in two optimum samples which were exfoliated separately with the assistance of two different stabilisers. AFM images of stabiliser Py-C_4-SASS assisted exfoliated graphene shows that the thickness of the majority of graphene flakes are around 2~4 nm, which indicate that most of the graphene are single and few layer graphene. Thickness analysis of AFM images confirms the Raman result, while the flake size distribution from the SEM images from two different samples shows that the graphene flake size (~ 0.5 μm) of Py-C_4-SASS assisted exfoliated is slightly larger than the other one (~ 0.2 μm).

In general, the absorbance of Py-C_4-SASS assisted exfoliated graphene suspension is almost twice as high as the Py-SASS assisted one. The designed stabiliser it gave two optimum performances at concentrations ~3 mg mL^{-1} and 7 mg mL^{-1}. The mechanism behind these two optimum performances still remains unknown. Moreover, the concentration is difficult to calculate since the extinction coefficient is variable when a different exfoliation agent is used. However, where C_s = 3 mg mL^{-1}, the graphene gravimetric concentrations $C_{(G,\ Py\text{-}C4\text{-}SASS)}$ are 1.01 mg mL^{-1}, while $C_{(G,\ Py\text{-}SASS)}$ is 0.41 mg mL^{-1}, which agree with the absorbance result. Therefore, Py-C_4-SASS gives higher graphene concentration than stabiliser Py-SASS in liquid phase graphene exfoliation.

Interestingly, computational molecular dynamic simulation indicated that the butyl spacer of the designed stabiliser lies flat on the surface of graphene rather than pointing into water. In addition, tensiometry result showed stabiliser Py-C_4-SASS occupied a smaller surface area than stabiliser Py-SASS in water since the butyl group has made the hydrophilic sulfonic acid salt end more flexible, so it can point into water more effectively. Although the simulation result and tensiometry result seem to contradict one another. As the computational experiment can only simulate the interaction of one infinite graphene flake and one stabiliser molecule in water medium while the surface tension measurement takes into account the behaviour of multiple stabilisers lowering the surface tension in water without the presence of graphene. Finally, two kinds of graphene dispersion with the assistance of different stabilisers were inkjet printed in order to measure the conductivity. It should be noted that when the height of the pattern is the same, the pattern printed from stabiliser Py-C_4-SASS assisted exfoliated graphene ink ($C_{(G,\ Py\text{-}C4\text{-}SASS)}$ ~ 0.8 mg mL^{-1}) has lower sheet resistance (83.76 kΩ/sq) than the pattern printed from stabiliser Py-SASS assisted exfoliated graphene ink ($C_{(G,\ Py\text{-}SASS)}$ ~ 0.4 mg mL^{-1}), whose sheet resistance is 170.21 kΩ/sq. Therefore, Py-C_4-SASS assisted exfoliated graphene ink could give better conductivity because it could give higher graphene concentration and relatively larger lateral size graphene flakes.

4.2 Further work

It is assumed the major source for error in A/l values of the designed stabiliser assisted exfoliated graphene suspensions are related to the insolubility of the stabiliser. It is noted in the experiment that the novel stabiliser could dissolve at high temperature when its concentration is lower than 4 mg mL^{-1}. Also, the stabiliser solution/suspension could remain stable (without large aggregation or precipitation) even when the temperature is reduced. Therefore, reducing the initial concentration of stabiliser may help to reduce the error bar as well. Moreover, for most of the stabiliser assisted liquid phase exfoliation of graphene studies,

the initial concentration of stabiliser is low (usually ≤ 1 mg mL^{-1}), yet the performance of some of them can still achieve high concentration for graphene dispersion. Hence, we are also keen to see whether the good performance of stabiliser could remain at low concentration.

In this project, a major unknown value is the concentration of the graphene dispersion. Since the method of determining the extinction coefficient is dependent on the gravimetric concentration of the graphene dispersion, yet as an intrinsic property, the extinction coefficient is independent. Thus, the concentration cannot be calculated via Beer-Lambert law. Therefore the gravimetric concentration measurement should be down for all dispersions, in order to find out the authentic graphene dispersion concentration.

The flake size distribution based on the SEM images provide an estimation for the size distribution, however for a more accurate and critical presentation, a flake size distribution calculated from TEM images over all graphene dispersion samples should be conducted to give a complete comparison of the performance over different stabiliser concentration. Furthermore, the thickness distribution of AFM images over all graphene dispersions is needed to calculate the yield by single layer graphene percentage Y_M.

As outlined in section 3.5-2, tip sonication is a technique whose drawback is lack of control; therefore the graphite cannot be exfoliated evenly. Moreover, as such a powerful technique, the graphene flake will be easily broken down into smaller flakes or holes and cleavages will be created. Shear force mixing technique could be tried in terms of scaling up the flake size and obtained high quality graphene flake.

In this project, owing to the limited time, the conductivity of inkjet-printed patterns is unknown because the height of them could not be measured. Hence, in the future experiment, the height of the pattern should be measured. Finally as mentioned in both section 1.4 and 3.6 that the presence of residual stabiliser molecule will affect the conductivity performance of

graphene, therefore the stabiliser molecule residual needs to be removed to enhance the conductivity of the printed pattern.

5. References

1. P. R. Wallace, *Phys. Rev.*, 1947, **71**, 622.
2. A. K. Geim and K. S. Novoselov, *Nature materials*, 2007, **6**, 183-191.
3. S. Morozov, K. Novoselov, M. Katsnelson, F. Schedin, D. Elias, J. Jaszczak and A. Geim, *Physical review letters*, 2008, **100**, 016602.
4. K. I. Bolotin, K. Sikes, Z. Jiang, M. Klima, G. Fudenberg, J. Hone, P. Kim and H. Stormer, *Solid State Communications*, 2008, **146**, 351-355.
5. X. Du, I. Skachko, A. Barker and E. Y. Andrei, *Nature nanotechnology*, 2008, **3**, 491-495.
6. S. Unarunotai, Y. Murata, C. E. Chialvo, N. Mason, I. Petrov, R. G. Nuzzo, J. S. Moore and J. A. Rogers, *Advanced Materials*, 2010, **22**, 1072-1077.
7. A. A. Balandin, *Nature materials*, 2011, **10**, 569-581.
8. I. Frank, D. M. Tanenbaum, A. Van der Zande and P. L. McEuen, *Journal of Vacuum Science & Technology B*, 2007, **25**, 2558-2561.
9. R. Faccio, P. A. Denis, H. Pardo, C. Goyenola and A. W. Mombrú, *Journal of Physics: Condensed Matter*, 2009, **21**, 285304.
10. F. Scarpa, S. Adhikari and A. S. Phani, *Nanotechnology*, 2009, **20**, 065709.
11. S. Brunauer, P. H. Emmett and E. Teller, *Journal of the American chemical society*, 1938, **60**, 309-319.
12. C. e. N. e. R. Rao, A. e. K. Sood, K. e. S. Subrahmanyam and A. Govindaraj, *Angewandte Chemie*, 2009, **121**, 7890-7916.
13. M. D. Stoller, S. Park, Y. Zhu, J. An and R. S. Ruoff, *Nano letters*, 2008, **8**, 3498-3502.
14. E. Yoo, J. Kim, E. Hosono, H.-s. Zhou, T. Kudo and I. Honma, *Nano letters*, 2008, **8**, 2277-2282.
15. R. S. Edwards and K. S. Coleman, *Nanoscale*, 2013, **5**, 38-51.
16. P. Sutter, *Nature Materials*, 2009, **8**, 171-172.
17. K. E. Whitener and P. E. Sheehan, *Diamond and Related Materials*, 2014, **46**, 25-34.
18. M. Lavin-Lopez, J. Valverde, M. Cuevas, A. Garrido, L. Sanchez-Silva, P. Martinez and A. Romero-Izquierdo, *Physical Chemistry Chemical Physics*, 2014, **16**, 2962-2970.
19. A. C. Ferrari, F. Bonaccorso, V. Fal'Ko, K. S. Novoselov, S. Roche, P. Bøggild, S. Borini, F. H. Koppens, V. Palermo and N. Pugno, *Nanoscale*, 2015, **7**, 4598-4810.
20. Y. Dappe, M. A. Basanta, F. Flores and J. Ortega, *Physical Review B*, 2006, **74**, 205434.
21. M. I. Katsnelson, *Materials today*, 2007, **10**, 20-27.
22. K. S. Novoselov, A. K. Geim, S. Morozov, D. Jiang, Y. Zhang, S. a. Dubonos, I. Grigorieva and A. Firsov, *Science*, 2004, **306**, 666-669.
23. L. Jiao, L. Zhang, X. Wang, G. Diankov and H. Dai, *Nature*, 2009, **458**, 877-880.
24. L. Valentini, *Diamond and Related Materials*, 2011, **20**, 445-448.
25. P. Kumar, L. Panchakarla and C. Rao, *Nanoscale*, 2011, **3**, 2127-2129.
26. S. Stankovich, D. A. Dikin, R. D. Piner, K. A. Kohlhaas, A. Kleinhammes, Y. Jia, Y. Wu, S. T. Nguyen and R. S. Ruoff, *carbon*, 2007, **45**, 1558-1565.
27. M. J. McAllister, J.-L. Li, D. H. Adamson, H. C. Schniepp, A. A. Abdala, J. Liu, M. Herrera-Alonso, D. L. Milius, R. Car and R. K. Prud'homme, *Chemistry of materials*, 2007, **19**, 4396-4404.
28. H. C. Schniepp, J.-L. Li, M. J. McAllister, H. Sai, M. Herrera-Alonso, D. H. Adamson, R. K. Prud'homme, R. Car, D. A. Saville and I. A. Aksay, *The Journal of Physical Chemistry B*, 2006, **110**, 8535-8539.

29. Y. Hernandez, V. Nicolosi, M. Lotya, F. M. Blighe, Z. Sun, S. De, I. McGovern, B. Holland, M. Byrne and Y. K. Gun'Ko, *Nature nanotechnology*, 2008, **3**, 563-568.
30. A. Ciesielski and P. Samorì, *Chemical Society Reviews*, 2014, **43**, 381-398.
31. J. N. Coleman, *Advanced Functional Materials*, 2009, **19**, 3680-3695.
32. F. Bonaccorso, A. Lombardo, T. Hasan, Z. Sun, L. Colombo and A. C. Ferrari, *Materials Today*, 2012, **15**, 564-589.
33. A. Ferrari, J. Meyer, V. Scardaci, C. Casiraghi, M. Lazzeri, F. Mauri, S. Piscanec, D. Jiang, K. Novoselov and S. Roth, *Physical review letters*, 2006, **97**, 187401.
34. L. Malard, M. Pimenta, G. Dresselhaus and M. Dresselhaus, *Physics Reports*, 2009, **473**, 51-87.
35. B. C. Brodie, *Philos. Trans. R. Soc. London*, 1859, **149**, 249-259.
36. U. Khan, A. O'Neill, M. Lotya, S. De and J. N. Coleman, *Small*, 2010, **6**, 864-871.
37. U. Khan, P. May, A. O'Neill and J. N. Coleman, *Carbon*, 2010, **48**, 4035-4041.
38. U. Khan, H. Porwal, A. O'Neill, K. Nawaz, P. May and J. N. Coleman, *Langmuir*, 2011, **27**, 9077-9082.
39. Y.-T. Liu, X.-M. Xie and X.-Y. Ye, *Carbon*, 2011, **49**, 3529-3537.
40. S. Barwich, U. Khan and J. N. Coleman, *The Journal of Physical Chemistry C*, 2013, **117**, 19212-19218.
41. M. M. Hossain, O.-K. Park, J. R. Hahn and B.-C. Ku, *Materials Letters*, 2014, **123**, 90-92.
42. L. Niu, M. Li, X. Tao, Z. Xie, X. Zhou, A. P. Raju, R. J. Young and Z. Zheng, *Nanoscale*, 2013, **5**, 7202-7208.
43. E.-Y. Choi, W. San Choi, Y. B. Lee and Y.-Y. Noh, *Nanotechnology*, 2011, **22**, 365601.
44. X. Zhang, A. C. Coleman, N. Katsonis, W. R. Browne, B. J. Van Wees and B. L. Feringa, *Chemical Communications*, 2010, **46**, 7539-7541.
45. C. M. Hansen, *Hansen solubility parameters: a user's handbook*, CRC press, 2007.
46. M. Yi, Z. Shen, S. Ma and X. Zhang, *Journal of Nanoparticle Research*, 2012, **14**, 1-9.
47. S.-L. Zhang, Z. Zhang and W.-C. Yang, *Applied Surface Science*, 2016, **360**, 323-328.
48. M. Lotya, Y. Hernandez, P. J. King, R. J. Smith, V. Nicolosi, L. S. Karlsson, F. M. Blighe, S. De, Z. Wang and I. McGovern, *Journal of the American Chemical Society*, 2009, **131**, 3611-3620.
49. J. M. Englert, J. Röhrl, C. D. Schmidt, R. Graupner, M. Hundhausen, F. Hauke and A. Hirsch, *Advanced Materials*, 2009, **21**, 4265-4269.
50. M. Lotya, P. J. King, U. Khan, S. De and J. N. Coleman, *ACS nano*, 2010, **4**, 3155-3162.
51. S. De, P. J. King, M. Lotya, A. O'Neill, E. M. Doherty, Y. Hernandez, G. S. Duesberg and J. N. Coleman, *Small*, 2010, **6**, 458-464.
52. L. Vaisman, H. D. Wagner and G. Marom, *Advances in colloid and interface science*, 2006, **128**, 37-46.
53. L. Zhang, Z. Zhang, C. He, L. Dai, J. Liu and L. Wang, *ACS nano*, 2014, **8**, 6663-6670.
54. X. An, T. Simmons, R. Shah, C. Wolfe, K. M. Lewis, M. Washington, S. K. Nayak, S. Talapatra and S. Kar, *Nano letters*, 2010, **10**, 4295-4301.
55. D. Parviz, S. Das, H. T. Ahmed, F. Irin, S. Bhattacharia and M. J. Green, *Acs Nano*, 2012, **6**, 8857-8867.
56. D.-W. Lee, T. Kim and M. Lee, *Chemical Communications*, 2011, **47**, 8259-8261.
57. H. Yang, Y. Hernandez, A. Schlierf, A. Felten, A. Eckmann, S. Johal, P. Louette, J.-J. Pireaux, X. Feng and K. Mullen, *Carbon*, 2013, **53**, 357-365.

58. A. Schlierf, H. Yang, E. Gebremedhn, E. Treossi, L. Ortolani, L. Chen, A. Minoia, V. Morandi, P. Samori and C. Casiraghi, *Nanoscale*, 2013, **5**, 4205-4216.
59. F. Irin, M. J. Hansen, R. Bari, D. Parviz, S. D. Metzler, S. K. Bhattacharia and M. J. Green, *Journal of colloid and interface science*, 2015, **446**, 282-289.
60. C. D. Williams and F. R. Siperstein, 2016.
61. K. W. J. Heard, Doctor of Philosophy PhD Thesis University of Manchester, 2016.
62. L. Bogani, C. Danieli, E. Biavardi, N. Bendiab, A. L. Barra, E. Dalcanale, W. Wernsdorfer and A. Cornia, *Angewandte Chemie*, 2009, **121**, 760-764.
63. A. J. Lampkins, E. J. O'Neil and B. D. Smith, *The Journal of organic chemistry*, 2008, **73**, 6053-6058.
64. L. Xie, X. Ling, Y. Fang, J. Zhang and Z. Liu, *Journal of the American Chemical Society*, 2009, **131**, 9890-9891.
65. B. Sun, Z. Dreger and Y. Gupta, *The Journal of Physical Chemistry A*, 2008, **112**, 10546-10551.
66. K. R. Paton, E. Varrla, C. Backes, R. J. Smith, U. Khan, A. O'Neill, C. Boland, M. Lotya, O. M. Istrate and P. King, *Nature materials*, 2014, **13**, 624-630.
67. V. Sanchez-Romaguera, M. A. Ziai, D. Oyeka, S. Barbosa, J. S. Wheeler, J. C. Batchelor, E. A. Parker and S. G. Yeates, *Journal of Materials Chemistry C*, 2013, **1**, 6395-6402.